Available online at www.sciencedirect.com
ScienceDirect
Lithos 102 (2008) 138–157
LITHOS
www.elsevier.com/locate/lithos

Large-scale Early Cretaceous volcanic events in the northern Great Xing'an Range, Northeastern China

Ji-Heng Zhang [a,b], Wen-Chun Ge [c], Fu-Yuan Wu [b,*], Simon A. Wilde [d], Jin-Hui Yang [b], Xiao-Ming Liu [e]

[a] State Key Laboratory of Geological Processes and Mineral Resources, College of Earth Sciences, China University of Geosciences, Wuhan 430074, China
[b] State Key Laboratory of Lithospheric Evolution, Institute of Geology and Geophysics, Chinese Academy of Sciences, P.O. Box 9825, Beijing 100029, China
[c] College of Earth Sciences, Jilin University, Jianshejie 2199, Changchun 130061, China
[d] Department of Applied Geology, Curtin University of Technology, P O Box U1987, Perth, Western Australia 6845, Australia
[e] State Key Laboratory of Continental Dynamics, Department of Geology, Northwest University, Xi'an 710069, China

Received 4 November 2006; accepted 6 August 2007
Available online 21 August 2007

Abstract

The Great Xing'an Range in northeastern China is characterized by large-scale Mesozoic magmatism, and forms a key part of the NE-trending Mesozoic magmatic belt in East China. However, only limited precise age data for the volcanic rocks in this belt were previously available, which significantly hampers understanding of the petrogenesis and geodynamic setting of these rocks. Systematic dating of volcanic rocks in the Great Xing'an Range was undertaken in order to rectify this situation. The Mesozoic volcanic rocks in the area have been sub-divided into the Tamulangou, Shangkuli and Yilieke formations. The Tamulangou and Yiliekede formations are composed of basalt and basaltic andesite, whereas the Shangkuli Formation consists of rhyolite and dacite. Zircon U–Pb and whole rock $^{40}Ar/^{39}Ar$ dating, combined with published data, indicate that the Tamulangou Formation was formed over a large time interval from the Early Jurassic to Early Cretaceous; it should therefore not be regarded as a single stratigraphic unit. In contrast, volcanic rocks of the Shangkuli and Yiliekede formations were erupted in the Early Cretaceous, between 125–115 Ma. Overall, most Mesozoic volcanic rocks in the Great Xing'an Range were erupted during the Early Cretaceous with an age peak at ~125 Ma, coeval with the time of lithospheric thinning in the eastern part of the North China Craton. Therefore, the Great Xing'an Range constitutes an important area that records a significant Early Cretaceous giant igneous event in eastern China. It is possible that this activity was related to subduction of the Pacific plate during the Late Mesozoic, as has been suggested to explain crustal thinning of the North China Craton.

Keywords: Geochronology; Volcanic rocks; Early Cretaceous; Great Xing'an Range; Northeastern China

1. Introduction

Mesozoic volcanic rocks and other associated igneous rocks are dominant in the Great Xing'an Range and adjacent areas of northeastern (NE) China, and constitute

* Corresponding author. Tel.: 86 10 62007392; fax: 86 10 62010846.
E-mail address: wufuyuan@mail.igcas.ac.cn (F.-Y. Wu).

0024-4937/$ - see front matter © 2007 Elsevier B.V. All rights reserved.
doi:10.1016/j.lithos.2007.08.011

one of the most striking geological features along the eastern Asian continental margin (Fig. 1). In the Great Xing'an Range, the Mesozoic volcanic rocks occur over an area of ~100,000 km^2. During the past decades, numerous studies have been conducted on these rocks (e.g. Jiang and Quan, 1988; Zhao et al., 1989; Ge et al., 2000, 2001; Lin et al., 2000, 2003; Shao et al., 2001a,b; Guo et al., 2001; Fan et al., 2003; Gao et al., 2005; Zhang et al., 2006). However, there has been much debate concerning the tectonic setting in which these rocks formed and several proposals have been put forward to explain the driving force for this magmatism, for example: (1) possible mantle plume activity or some other intraplate process (Shao et al., 1994, 2001a,b; Deng et al., 1996; Lin et al., 1998; Ge et al., 1999), (2) subduction of the Mongol–Okhotsk Ocean from the north (Fan et al., 2003; Meng, 2003), and (3) subduction of the Paleo-Pacific plate from the east (Jiang and Quan, 1988; Zhao et al., 1989).

The main reason for the above conflict is that the exact eruption ages of the volcanic rocks was unknown and their spatial distribution had not been previously determined. It was earlier considered that volcanic rocks in this region were erupted during the Middle Jurassic to Early Cretaceous based on K–Ar, Rb–Sr and a small number of U–Pb ages (Jiang and Quan, 1988; Zhao et al., 1989; Wang et al., 1997; IMBGMR, 1991; HBGMR, 1993; Fan et al., 2003). However, some of these ages should be regarded as suspect. For example, the low closure temperature makes the K–Ar dates unreliable, since rocks in the region have undergone intense alteration and weathering. Similarly, the narrow range of Rb/Sr isotopic ratios yields large errors in the Rb–Sr isochron ages. From the published data, the only reliable Rb–Sr isochron age is that for the Shangkuli pantellerite from Hulun Lake in the northern Great Xing'an Range (127±5 Ma, Ge et al., 2001). Finally, very few zircon U–Pb isotopic ages have been published from this area, although some discordant ages have been reported for volcanic rocks in the south Great Xing'an Range (Zhao et al., 1989). Recently, several Ar–Ar ages have

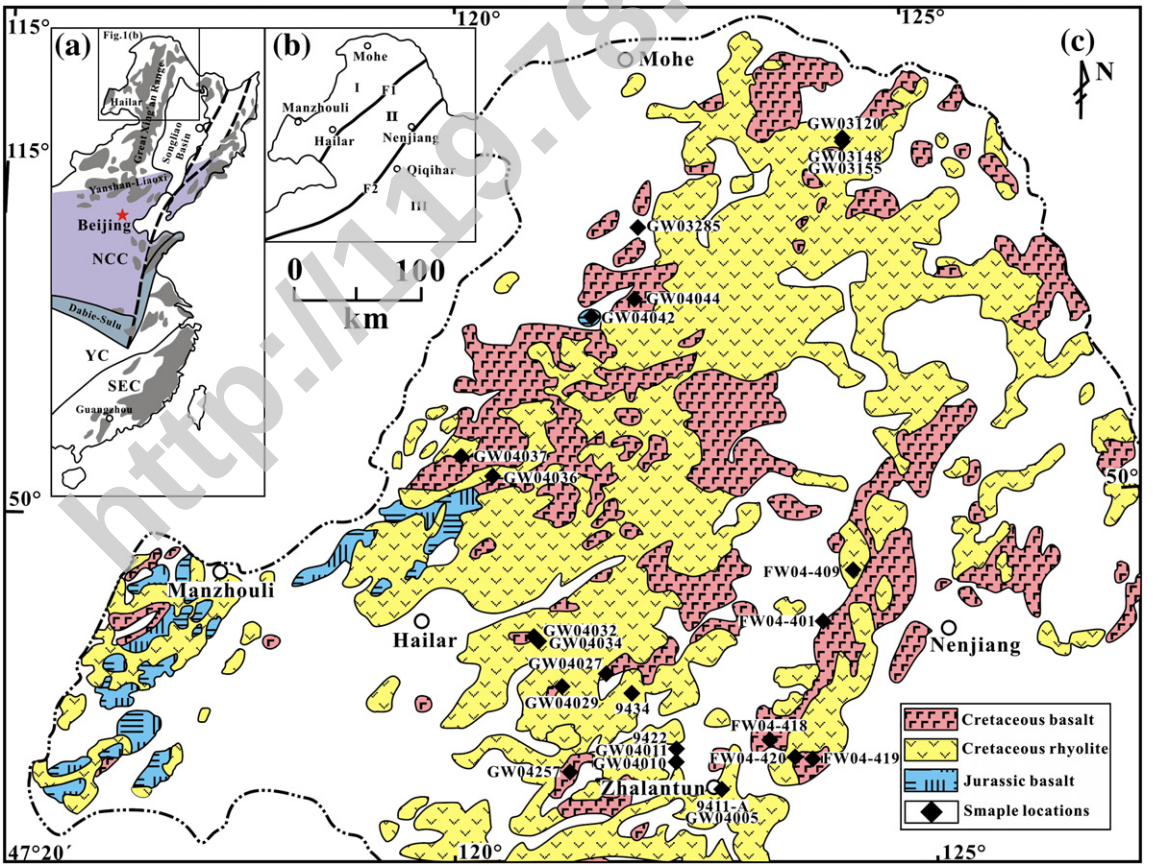

Fig. 1. (a) Simplified tectonic units of eastern China. NCC: North China Craton; YC: Yangtze Craton; SEC: South East China. (b) Tectonic subdivisions of northeastern China. F1: Tayuan–Xiguitu Fracture Belt; F2: Nenjiang–Hegenshan Fracture Belt. I: Ergun Block; II: Xing'an Block; III: Songnen Block. (c) Distribution of Mesozoic volcanic rocks in the Great Xing'an Range, showing sample locations.

been reported by Wang et al. (2006) and Wu G. et al. (2006) from just a small part of the range. Therefore, systematic dating on the huge area of volcanic rocks in the Great Xing'an Range is urgently required, in order to determine when volcanism took place and to evaluate the mechanism which drove the magmatism, i.e., how such a huge volume of magma was generated.

In this paper, we report high precision zircon U–Pb and whole-rock Ar–Ar geochronological data for the volcanic rocks exposed in the northern Great Xing'an Range of NE China (Fig. 1). The data are then used to evaluate the variety of models proposed to explain the tectonic setting,, in particular, whether lithospheric thinning took place in NE China.

2. Geological setting

Eastern China is composed of the Xing'an–Mongolian Orogenic Belt (XMOB), representing the eastern extension of the Central Asian Orogenic Belt, and the North China Craton (NCC) in the north, the Dabie–Sulu ultrahigh-pressure collisional belt in the central part, and the Yangtze Craton (YC) and Southeastern (SE) China Orogenic Belt in the south (Fig. 1a). The Great Xing'an Range (named Da Hinggan Mountains in some of the literature) is located in the western part of the XMOB in NE China. This region is composed of the Erguna, Xing'an and Songnen blocks, separated by the Tayuan–Xiguitu and Nenjiang–Hegenshan faults (Ye et al., 1994; Fig. 1b). The Erguna Block, considered to be the eastern extension of the Central Mongolian microcontinent, is located in the northwestern part of the region (Fig. 1). Its geological evolution is largely unknown, as the area is heavily forested, although the block is considered to be composed of Proterozoic to Palaeozoic strata and granites (HBGMR, 1993), yet few reliable geochronological data are available. More recent work indicates that Early Paleozoic granitic magmatism is well developed in the area (Ge et al., 2005a; Wu et al., 2005c). The Xing'an Block, located in the Great Xing'an Range, is characterized by extensive Mesozoic volcanic and granitic rocks, although some are now known to have formed in the Paleozoic (Fan et al., 2003; Wu et al., 2002; Ge et al., 2005a), especially in the southern part. Previously identified Proterozoic metamorphic rocks (HBGMR, 1993), are now considered to be Paleozoic in age, based on recent geochronology (Miao et al., 2004). The Songnen Block is mostly represented by the Songliao sedimentary basin. Its eastern and northern parts are the Zhangguangcai and Lesser Xing'an Ranges which are characterized by voluminous Mesozoic granitic rocks, with rare Paleozoic strata occurring as remnants in a granitic 'ocean' (Wu et al., 2000b). Recent borehole data from the Songliao Basin reveal that granites are widespread (Wu et al., 2001).

During the Phanerozoic, this area underwent a complex evolutionary history, characterized by multiple stages of accretion and collision (Sengör et al., 1993). Based on the discovery of ophiolitic complexes along the Tayuan–Xiguitu Fault and development of Early Ordovician post-orogenic granites (Yan et al., 1989; Zhang and Tang, 1989; Li, 1991; Ge et al., 2005a), it is proposed that the Erguna Block collided with the Xing'an Block during the Early Paleozoic. The Songliao Block was then accreted to the Xing'an–Erguna composite block along the Hegenshan–Heihe suture in the Late Devonian to Early Carboniferous (Ye et al., 1994; Hong et al., 1994; Robinson et al., 1999; Chen et al., 2000; Sun et al., 2001; Wu et al., 2002; Zhou et al., 2003, 2005; Shi et al., 2004). Subsequently, regional extension developed in the late Palaeozoic (Tang, 1990).

During Mesozoic time, the Great Xing'an Range was affected by the widespread emplacement of Late Mesozoic volcanic and granitic rocks (Lin et al., 2004; Ge et al., 2005b). Recent studies indicate that the Mesozoic granites, along with those of Paleozoic age, represent significant juvenile crustal addition, since these granites show positive $\varepsilon_{Nd}(t)$ values and young Nd model ages (Jahn et al., 2000; Wu et al., 2000b, 2002).

3. Mesozoic volcanic rocks in the northern Great Xing'an Range

Mesozoic volcanic rocks cover an area of ~100,000 km^2 in the Great Xing'an Range (Fig. 1c). In this study, we focus on the northern segment, which extends into Heilongjiang Province in the east and the Inner Mongolia Autonomous Region in the west. These Mesozoic volcanic rocks have been classified into several stratigraphic schemes, which unfortunately change in different locations or with different researchers (Jiang and Quan, 1988; Zhao et al., 1989; IMBGMR, 1991; HBGMR, 1993). In Inner Mongolia, the volcanic rocks were subdivided, in stratigraphic order from bottom to top, into the Tamulangou, Shangkuli and Yiliekede formations (IMBGMR, 1991); whereas in Heilongjiang Province, they were subdivided into the Tamulangou, Longjiang, Guanghua and Ganhe formations (HBGMR, 1993). Based on a broader lithological correlation, the former subdivision was favoured by Wang et al. (1997) (see Fig. 2a) and this has become widely accepted, including in this study. The volcanic rocks unconformably overlie clastic sedimentary rocks of the Nanping Formation, which is Jurassic in age (Wang

Formation	Thickness	Rock type
Yiliekede	10-306 m	Basalt, basalt-andesite
Shangkuli	100-1421 m	Dacite-rhyolite
Murui	21-187 m	Sedimentary rocks
Tamulangou	>1218 m	Basalt, basalt-andesite
Nanping		Sedimentary rocks

Fig. 2. (a) Stratigraphic subdivisions of the Mesozoic rocks in the northern Great Xing'an Range (After Wang et al., 1997).

et al., 1997). However, the above four-fold subdivision into formations, which includes the occurence of the Murui Formation between the Tamulangou and Shangkuli formations, has never been observed in a single section, which makes their relationship questionable in some locations, since it was established by lithological comparisons.

The Tamulangou Formation is poorly exposed and located in the western part of the area (Fig. 1c) and is mainly composed of basalts and basaltic andesites with some rhyolitic tuffs. The rocks contain various percentages of phenocrysts, which are mainly composed of plagioclase, pyroxene and local olivine: most phenocrysts are altered. In addition, some rocks are massive without any phenocrysts. Amygdaloidal structures are also a common feature, and many are filled with agate or calcite.

The Shangkuli Formation is composed mainly of rhyolite and dacite and related volcanoclastic rocks and is the major rock unit in the area. The rhyolites and dacites mostly have a porphyritic texture, with phenocrysts set in a felsitic matrix; flow, spherulitic and perlitic structures are common. The phenocrysts are mainly sanidine, quartz, plagioclase and biotite. Locally, alkali rhyolites, geochemically similar to A-type granites, are present (Ge et al., 2001).

The Yiliekede Formation is widely distributed, although less extensive than the Shangkuli Formation, and mainly consists of basalt and basaltic-andesite, with ophitic or vitrophyric textures. Variable concentrations of olivine and plagioclase phenocrysts can be observed within a matrix of plagioclase, olivine, clinopyroxene, and locally brown basaltic glass. Olivine occurs either as phenocrysts or in the matrix, but rarely both, and has been extensively altered to iddingsite. Amygdaloidal structures are common.

In the TAS (SiO_2–Na_2O+K_2O) classification diagram (Fig. 3), these volcanic rocks straddle the alkaline-subalkaline boundary and plot as basalt, basaltic-andesite, andesite, dacite, rhyolite, trachy-andesite, as well as trachyte and more alkaline types. Geochemically (Jiang and Quan, 1988; Zhao et al., 1989; Ge et al., 2000, 2001; Lin et al., 2000, 2003; Shao et al., 2001a,b; Guo et al., 2001; Fan et al., 2003; Gao et al., 2005; Zhang et al., 2006), the volcanic rocks possess similar rare earth element (REE) patterns, but with variable amounts of HREE depletion and variable negative Eu anomalies. The trace element patterns show a relatively strong depletion of Nb, Ta, P and Ti, and a wide range in Rb, Ba and Sr values. Some of the rocks possess high Ba and Sr and low Y, typical features of adakitic rocks. These rocks also show relatively homogeneous Sr–Nd isotopic compositions, the same as the granite in the area, with low $(^{87}Sr/^{86}Sr)_i$ ratios and positive $\varepsilon_{Nd}(t)$ values (Ge et al., 2001; Fan et al., 2003).

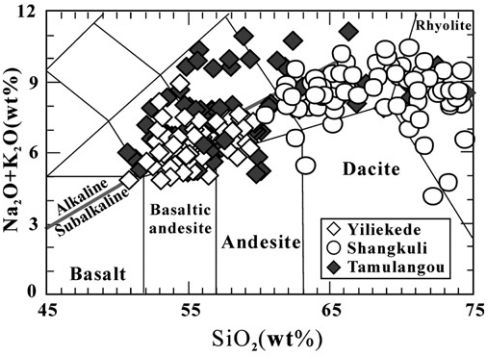

Fig. 3. Na_2O+K_2O v. SiO_2 variation diagram showing the rock types of the Tamulangou, Shangkuli and Yiliekede formations. The boundary between alkaline and subalkaline is from Irvine and Baragar (1971). Data sources: Jiang and Quan (1988), IMBGMR (1991), HBGMR (1993), Ge et al. (1999, 2000, 2001); Lin et al. (2000, 2003).

As noted above, the Mesozoic volcanic rocks in the Great Xing'an Range were previously thought to be erupted during the Middle Jurassic to Early Cretaceous, based on a few isotopic ages (Jiang and Quan, 1988; Zhao et al., 1989; Wang et al., 1997; IMBGMR, 1991; HBGMR, 1993). However, most of these cited ages were determined by the K–Ar method, which is notoriously susceptible to disturbance. Although some high precision Ar–Ar isotopic ages have been published recently (Wu et al., 2005b; Wang et al., 2006), they are inadequate for determining the overall picture of Mesozoic magmatism in the area. In order to obtain such data, we undertook a comprehensive sampling program of zircon U–Pb dating, including 13 felsic volcanic rocks (rhyolite, dacite and rhyolitic tuff), 5 mafic volcanic rocks (basalt and andesite) and 3 related dykes (dolerite and porphyry). Sample crushing and zircon selection were undertaken by the Geological Laboratory of the Hebei Regional Geology Survey Team at Langfang, following standard heavy liquid and magnetic separation techniques. Because mafic rocks commonly contain too few zircons to analyse, 4 basalts were also selected for whole-rock $^{40}Ar/^{39}Ar$ analysis using the incremental heating technique. The sample locations are listed in Table 1.

4. Analytical techniques

4.1. TIMS analyses

Single grain zircon U–Pb ages for samples 9422 and 9436 (rhyolitic tuff) from the central Great Xing'an Range were obtained using a VG 354 thermal ionization mass spectrometer (TIMS), fitted with a Daly collector, at the Tianjin Institute of Geology and Mineral Resources, Chinese Academy of Geological Sciences. The procedure for zircon dissolution and U–Pb chemical separation can be found in Li et al. (1995) and references therein. A ^{205}U–^{235}U spike was added to the zircon samples in a 0.25 mL fluorine-plastic capsule for zircon dissolution. The final isolated U and Pb were loaded onto a Re filament with silica gel-phosphoric acid. All U and Pb data were corrected for mass fractionation. The blanks were 0.05 ng for Pb and 0.002 ng for U. The obtained isotopic ratios and the age data are reported at the 2σ level.

4.2. LA-ICPMS analyses

Grains of transparent, euhedral, unfractured and inclusion-free zircon were hand-picked under a binocular

Table 1
Zircon U–Pb and whole-rock Ar–Ar isotopic ages for the Mesozoic volcanic rocks in the Great Xing'an Range, NE China

Sample no.	Locations	Latitude and longitude	Formation	Rock type	Age (Ma)	Method
GW03285	Mangui	52°03′27″N, 122°05′33″E	Dyke	Dolerite	133±3	LA-ICPMS
9411-A	Zhalantun	48°00′12″N, 122°46′19″E	Dyke	Granite–Porphyry	130±1	LA-ICPMS
GW04005	Zhalantun	48°00′12″N, 122°46′19″E	Dyke	Coarse dolerite	124±2	LA-ICPMS
FW04-420	Langdonggou	48°16′31″N, 123°38′12″E	Yilikede Fm.	Basaltic andesite	123±2	LA-ICPMS
GW03120	Walagan–Mengkeshan	52°39′39″N, 124°19′42″E	Yilikede Fm.	Basalt	126±5	LA-ICPMS
GW04027	Yilikede	48°51′11″N, 121°37′27″E	Yilikede Fm.	Basalt	112.2±2.1	^{40}Ar–^{39}Ar
GW04032	Mianduhe	49°07′01″N, 120°55′43″E	Yilikede Fm.	Basalt	117.5±1.3	^{40}Ar–^{39}Ar
FW04-401	Nuomin	49°14′31″N, 123°46′04″E	Shangkuli Fm.	Andesite	123±1	LA-ICPMS
FW04-409	Yilizhen	49°34′00″N, 124°14′18″E	Shangkuli Fm.	Rhyolite	118±2	LA-ICPMS
FW04-418	Huoerqi	48°23′02″N, 123°19′28″E	Shangkuli Fm.	Dacite	113±2	LA-ICPMS
FW04-419	Anjiatun	48°15′45″N, 123°45′47″E	Shangkuli Fm.	Dacite	116±1	LA-ICPMS
GW04029	Gaojishanlinchang	48°48′05″N, 121°09′32″E	Shangkuli Fm.	Rhyolite	119±2	LA-ICPMS
GW04034	Mianduhe	49°07′15″N, 120°54′22″E	Shangkuli Fm.	Rhyolite	111±1	LA-ICPMS
GW04036	Shangkuli	50°14′47″N, 120°28′08″E	Shangkuli Fm.	Rhyolite	119±2	LA-ICPMS
GW04044	Niuerhe	51°32′04″N, 122°01′08″E	Shangkuli Fm.	Rhyolite-Porphyry	135±1	LA-ICPMS
GW03148	Pangu	52°38′27″N, 124°41′09″E	Shangkuli Fm.	Rhyolite	128±1	LA-ICPMS
GW03155	Pangu	52°38′27″N, 124°41′09″E	Shangkuli Fm.	Rhyolite	125±1	LA-ICPMS
GW04037	Sanhezhen	50°26′04″N, 120°08′59″E	Tamulangou Fm.	Olivine basalt	139±2	LA-ICPMS
GW04037	Sanhezhen	50°26′04″N, 120°08′59″E	Tamulangou Fm.	Olivine basalt	139.9±1.8	^{40}Ar-^{39}Ar
9434	Boketu	48°44′12″N, 121°55′20″E	Tamulangou Fm.	Rhyolitic tuff	139±1	TIMS
9422	Balin Station	48°17′57″N, 122°19′09″E	Tamulangou Fm.	Rhyolitic tuff	141±4	TIMS
GW04010	Nanmu	48°13′01″N, 122°20′37″E	Tamulangou Fm.	Rhyolitic tuff	146±2	LA-ICPMS
GW04011	Balin Station	48°17′57″N, 122°19′09″E	Tamulangou Fm.	Rhyolitic tuff	148±2	LA-ICPMS
GW04257	Tamulangou	48°09′13″N, 121°14′44″E	Tamulangou Fm.	Basalt	128±8	LA-ICPMS
GW04042	Tamulangou	51°25′56″N, 121°31′52″E	Tamulangou Fm.	Basalt	186.3±2.8	^{40}Ar–^{39}Ar

microscope and then mounted in epoxy resin for LA-ICPMS (Laser Ablation Inductively Coupled Plasma Mass Spectrometry) U–Pb isotopic analyses. The mounts were polished in order to section the grains in half, and cathodoluminescence (CL) images were then taken in order to reveal the inner structure of the grains and to enable selection of the best domains to undertake U–Pb isotopic analysis. The CL images were obtained at the Electron Microprobe Laboratory at the Institute of Geology and Geophysics, Chinese Academy of Sciences, Beijing.

Although the LA-ICPMS technique was only developed in the last decade, recent studies have shown it to be a powerful tool in geochronology (Liu et al., 1998; Liang et al., 2000; Ballard et al., 2001; Harris et al., 2004; Jackson et al., 2004; Yuan et al., 2004). The main problem with the method is mass discrimination and isotopic fractionation during ablation and transportation. Generally, the precision of individual spots using LA-ICPMS is inferior to that of TIMS and SHRIMP, but it has been greatly improved by the external correction using standard zircons (Black et al., 2004). Many studies indicate that even for Phanerozoic zircons, the data obtained by LA-ICPMS are consistent with that obtained by TIMS or SHRIMP (Ballard et al., 2001; Li et al., 2001; Harris et al., 2004; Jackson et al., 2004; Yuan et al., 2004). Although this method is not precise enough for time calibration, the rapid analysis at low cost means the technique is cost-effective. In this study, LA-ICPMS U–Pb isotope analyses were conducted at the State Key Laboratory of Continental Dynamics of Northwest University, Xi'an. An Agilent 7500 a, connected with a 193 nm ArF excimer laser ablation system, was employed to do the analyses. The NIST synthetic silicate glass standard reference material NIST SMR610 was used to optimize the instrument, and the international reference standard zircon 91500 was used as the external standard for the age calibration. During the analyses, highly pure helium gas was used to transfer the ablated materials. The spot size was 30μm and detailed procedures and methods, as well as the parameters of the instrument, can be found in Yuan et al. (2004). The GLITTER (Ver. 4.0 Macquarie University, Jackson et al., 2004) and Isoplot (Ver. 3.0, Ludwig, 2003) programs were used to calculate the isotope ratios and ages, respectively. Common lead was calculated by the method of Andersen (2003). Because these volcanic rocks were erupted during the Phanerozoic, the $^{206}Pb/^{238}U$ ages were used to define the formation age of the rocks. Single spot data are reported at the 1σ level, whereas, the weighted mean ages are calculated at the 95% confidence level (2σ).

4.3. $^{40}Ar/^{39}Ar$ analyses

The $^{40}Ar/^{39}Ar$ method can be used to determine the age of fine-grained volcanic rocks and selected single minerals, and is particularly suitable for fine-grained mafic volcanic rocks, for which the zircon U–Pb dating is normally inappropriate. During analysis, ^{39}Ar and ^{40}Ar can be measured simultaneously by the same instrument so that heterogeneity in the sample, as well as system errors, can be effectively reduced (Wang et al., 2006). Using the data obtained by incremental heating, the isochron age of a single sample can be obtained and the initial $^{36}Ar/^{40}Ar$ isotopic ratio revealed.

Four fine-grained basalts were dated using the $^{40}Ar/^{39}Ar$ incremental heating technique. In order to constrain the eruption age and avoid excess argon, 60–80 mesh granules of processed groundmass were carefully hand-picked under a binocular microscope. The $^{40}Ar/^{39}Ar$ dating was performed at the Geochronology Laboratory in the Institute of Geology and Geophysics, Chinese Academy of Sciences, Beijing; the analytical protocol follows Wang et al. (2005).

Groundmass wafers weighing between 3.5–4.0 mg, together with multiple samples of the 18.6±0.4 Ma neutron fluence monitor mineral Brione muscovite (Flisch, 1982) were irradiated *in vacuo* within a cadmium-coated quartz vial for 45.8 h in position H8 at the Beijing Atomic Energy Research Institute reactor (49–2). A number of neutron fluence monitors (standards) have been intercalibrated at the Institute of Geology and Geophysics, Chinese Academy of Sciences (Wang et al., 2005). Replicate (6–8) analyses of the monitors from each position in the vials constrain the vertical neutron flux gradient to within ±0.7% and this additional uncertainty is propagated into the plateau and isochron ages. Relative to 18.6 Ma Brione muscovite monitor, 9 total fusion analyses of Mt Dromedary (New South Wales, Australia) biotite (GA-1550), gave a mean age of 98.5± 0.6 Ma, consistent with the 98.5±0.8 Ma and 98.8 ± 0.5 Ma ages determined by Spell and McDougall (2003) and Renne et al. (1998), respectively. Interfering nucleogenic reactions were checked for every irradiation by using CaF and K_2SO_4. Mass discrimination is monitored by using an on-line air pipette, from which multiple measurements are made before and after each incremental-heating experiment.

Groundmass wafers were placed into a Ta tube resting in the Ta crucible of an automated double-vacuum resistance furnace and incrementally-heated in 15 steps at 10 minutes intervals from 700 °C or 750 °C to 1500 °C. Following 5 additional minutes of gas purification on Al–Zr getters, isotopic measurements were made on a MM5400 mass spectrometer with a Faraday cup and an

electron multiplier. Hot system blanks were determined several times each day prior to degassing, which were commonly 2–3 orders of magnitude smaller than sample signals. Although the mean blank errors were generally ~2% for ^{40}Ar and ~5% for ^{36}Ar, the large size of the samples relative to the blank minimized the impact of propagating these errors into the final age calculations.

Plateau ages were determined from 3 or more contiguous steps, comprising >50% of the ^{39}Ar released, and gave concordant ages at the 95% confidence level. Errors are reported at the 2σ confidence level.

5. Results

The isotopic data, including zircon LA-ICPMS, TIMS and whole-rock Ar–Ar, are listed in the Eletronic Annexes 1, 2 and 3. Representative CL images of the analyzed zircons are presented in Fig. 4.

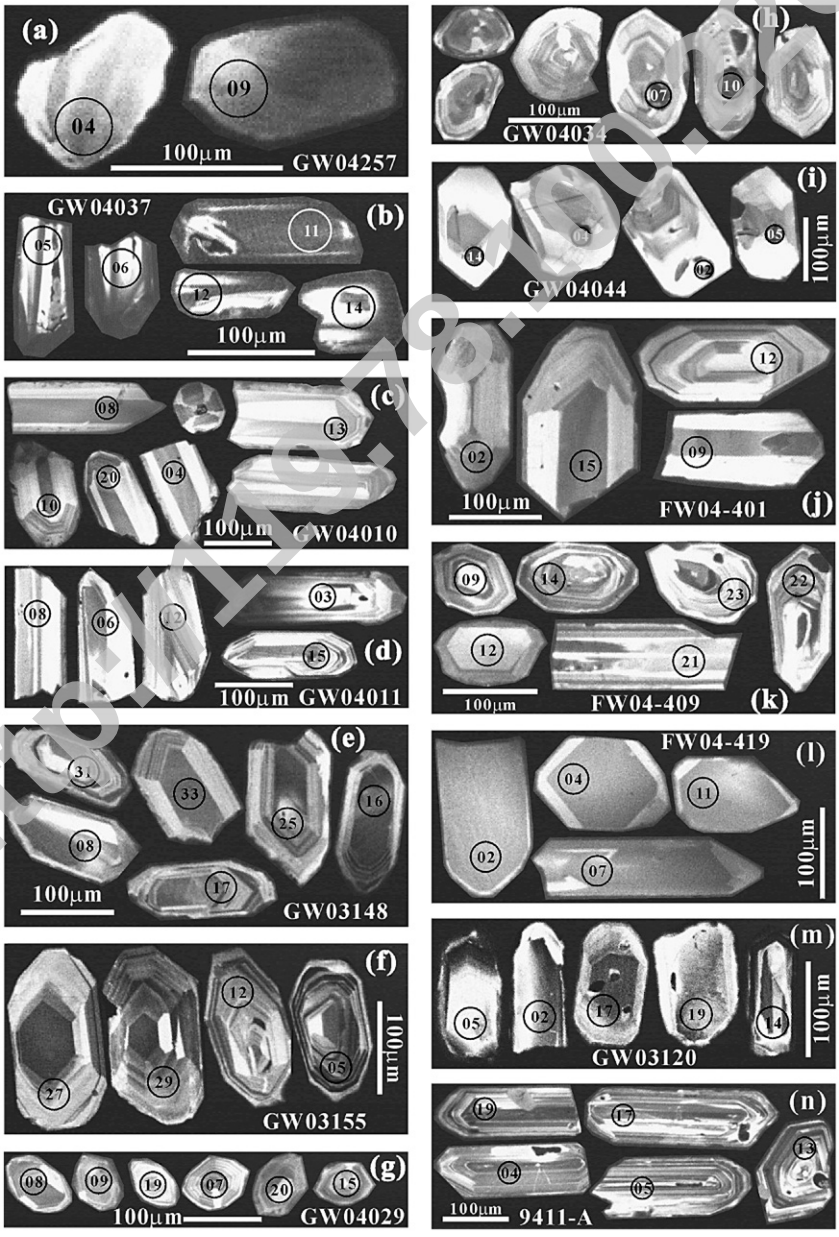

Fig. 4. Representative CL images of analyzed zircons from the Mesozoic volcanic rocks in the northern Great Xing'an Range.

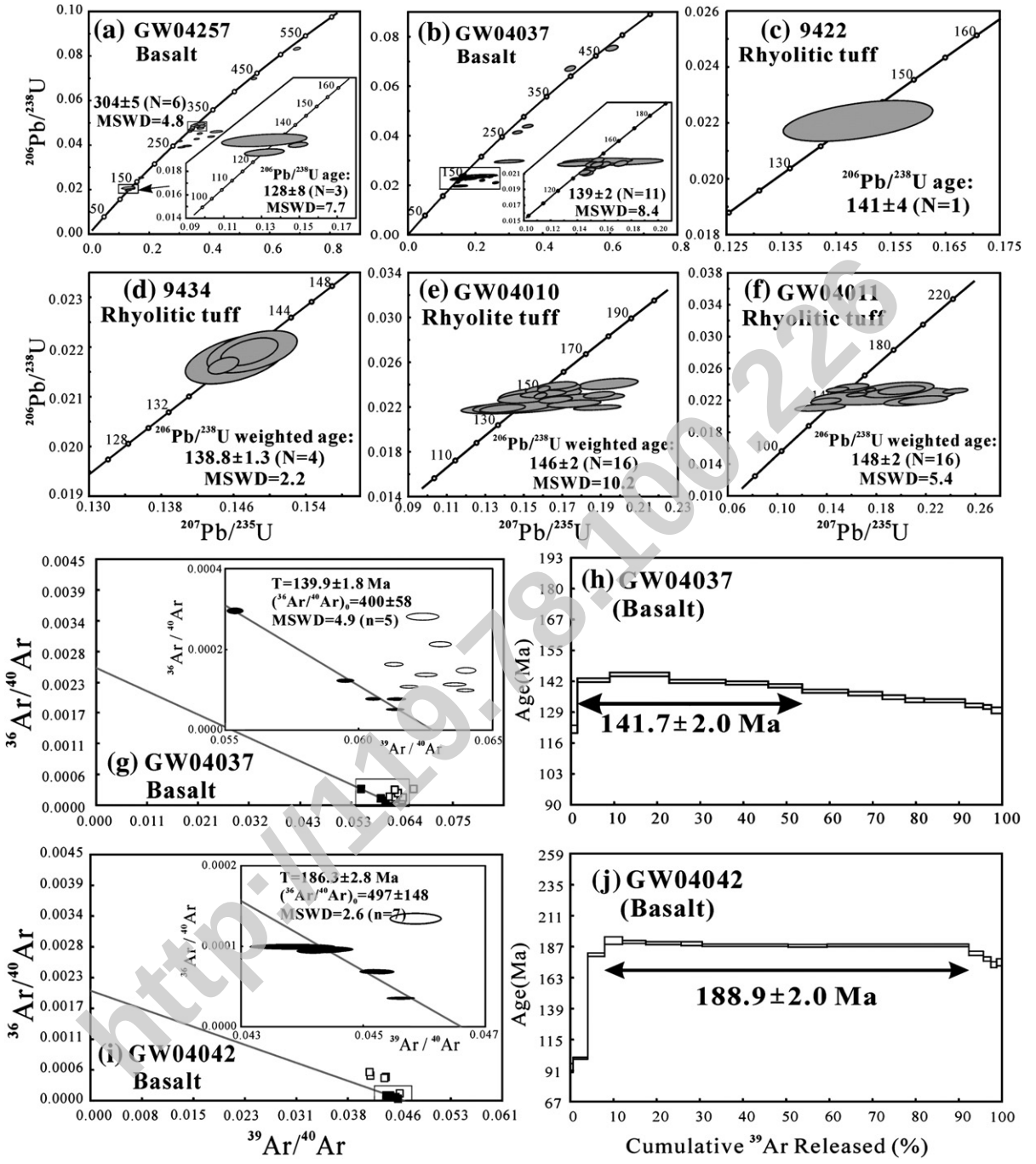

Fig. 5. Geochronological diagrams of the Tamulangou basalts. (a) sample GW04257 (zircon LA-ICPMS), (b) sample GW04037 (zircon LA-ICPMS), (c) sample 9422 (zircon TIMS), (d) sample 9434 (zircon TIMS), (e) sample GW04010 (zircon LA-ICPMS), (f) sample GW04011 (zircon LA-ICPMS), (g) and (h) sample GW04037 (whole-rock Ar–Ar), and (i) and (j) sample GW04042 (whole-rock Ar–Ar).

5.1. Tamulangou Formation

Being the lowest volcanic unit in the Great Xing'an Range, the eruption age of the Tamulangou Formation is vital in order to constrain the onset of Mesozoic volcanism in the area. In our study, three basalts and four rhyolitic tuffs were selected for LA-ICPMS, TIMS and $^{40}Ar/^{39}Ar$ dating; among these, sample GW04257 was collected from the original location where the Tamulangou Formation was established. The basalts are all

porphyritic, containing phenocrysts of plagioclase; some also contain phenocrysts of altered olivine and pyroxene. Amygdales are ubiquitous except in sample GW04042.

Zircons from sample GW04257 (basalt) show a complex age pattern. Most of them define a concordant age of 304±5 Ma (MSWD=4.8). This age may represent zircon grains extracted from the wall rock or else from the magma source. Three younger zircon grains (Fig. 4a), plotting on or near concordia (Fig. 5a), yield a $^{206}Pb/^{238}U$ age of 128± 8 Ma (MSWD=7.7), which is interpreted as the age of crystallization of the rock. Sample GW04037 is an olivine basalt, with some grains of olivine altered to iddingsite. Eleven analyses give a concordant $^{206}Pb/^{238}U$ age of 139±2 Ma (MSWD=8.4) (Fig. 5b). The morphology and oscillatory zoning or homogeneous inner structure of the grains (Fig. 4b) suggests a magmatic origin and this age is taken as the crystallizationage of the rock.

Four tuffs from the Tamulangou Formation were dated using both the TIMS (samples 9422 and 9434) and LA-ICPMS (samples GW04010 and GW04011) methods. They are all porphyritic, with some crystal fragments of plagioclase and quartz, as well as some biotite. One TIMS analysis of a transparent euhedral crystal from sample 9422 gave a concordant $^{206}Pb/^{238}U$ age of 141±4 Ma (Fig. 5c); whereas, 4 analyses of transparent euhedral crystals from sample 9434 define a weighted mean $^{206}Pb/^{238}U$ age of 138.8±1.3 Ma (MSWD=2.2) (Fig. 5d). Both ages are taken to represent the eruption time of the rocks, since the zircon crystals are euhedral in shape, suggesting a magmatic origin. The other two rhyolitic tuffs were dated by the LA-ICPMS method. Sixteen analyses of zircons from sample GW04010 define a concordant $^{206}Pb/^{238}U$ age of 146±2 Ma (MSWD=10.2) (Fig. 5e). Although some analyses are dispersed away from concordia, all 16 analyses of zircon from sample GW04011 define a weighted mean $^{206}Pb/^{238}U$ age of 148± 2 Ma (MSWD=5.4) (Fig. 5f). The zircons from both samples are euhedral in shape and show oscillatory zoning in CL image (Fig. 4c &d), indicating these ages represent the magmatic crystallization age of the rocks.

In order to check the reliability of the zircon dating of the basalts, sample GW04037 was also dated using the $^{40}Ar/^{39}Ar$ method (Fig. 5g &h). Because of alteration of phenocrystic olivine, excess Ar is present in the rock and affected the isotopic data. However, five homogeneous steps define an inverse isochron curve and record an age of 139.9±1.8 Ma (MSWD=4.9) (Fig. 5g), with an initial $^{36}Ar/^{40}Ar$ ratio of 400±58, and a plateau age of 141.7± 2.0 Ma (Fig. 5h). Both of these are consistent with the zircon U–Pb age. Sample GW04042 is a massive basalt that contains a few phenocrysts of altered plagioclase. The first 3 steps give an anomalously young plateau age, probably caused by recoil of ^{39}Ar during the irradiation or surficial ^{40}Ar. Nevertheless, the following 7 homogeneous steps give a plateau age of 188.9±2.0 Ma (Fig. 5j), and the inverse isochron age of these 7 steps is 186.3±2.8 Ma (MSWD=2.6), with an initial $^{36}Ar/^{40}Ar$ ratio of 497±148 (Fig. 5i). The relatively large uncertainty of the initial ratio may be attributed to the affect of the altered phenocrysts. The age of 186.3 ± 2.8 Ma is considered to be the crystallization age of the rock.

5.2. Shangkuli Formation

The Shangkuli Formation is mainly composed of felsic volcanic rocks, with some interlayered intermediate volcanic rocks, and forms the bulk of the volcanic rocks in the Great Xing'an Range. Fourteen samples, including rhyolite, dacite, andesite and rhyolitic tuff, were selected for LA-ICPMS and TIMS analyses. Most of these rocks have a porphyritic texture, with sanidine and quartz the most common phenocrysts in the rhyolite and rhyolite porphyry, while plagioclase is the most abundant phenocryst in the dacite and andesite; biotite is also commonly present. The rocks show felsitic and/or hyaline texture and some spherulitic textures can also be observed.

The 10 rhyolitic and dacitic lavas were dated by LA-ICPMS, since they contained enough zircons for U–Pb analyses. The selected zircons are mostly euhedral with oscillatory zoning (Fig. 4e–l). Samples GW03148 and GW03155 were both collected in the far north of the Great Xing'an Range, and the weighted mean $^{206}Pb/^{238}U$ ages are 128±1 and 125±1 Ma (Fig. 6a and b), respectively. These ages are considered to record the eruption time of the rocks. Nineteen analyses of zircon grains from sample GW04029, a massive rhyolite, yield a concordant age of 119±2 Ma (MSWD=8.9) (Fig. 6c). The analyses are concentrated on or near concordia, and are taken to represent the crystallization age of the rhyolite. Sample GW04034, collected from the uppermost layer of the Shangkuli Formation, has a weighted mean $^{206}Pb/^{238}U$ age of 111±1 Ma from 15 analyses (Fig. 6d). Sample GW04036, collected from the location where the Shangkuli Formation was first established, shows a vitreous texture. Sixteen analyses yield a concordant age of 119±2 Ma (MSWD=9.2) (Fig. 6e). Sample GW04044 is a rhyolitic porphyry, and 22 analyses are concordant and yield a weighted mean $^{206}Pb/^{238}U$ age of 135±1 Ma (MSWD=1.0) (Fig. 6f).

The following four samples were collected from the eastern part of the Great Xing'an Range. Sample

FW04-401 is a hornblende-bearing andesite with plagioclase, dark-rimmed hornblende and biotite as the phenocryst phases. Twenty one analyses yield a weighted mean $^{206}Pb/^{238}U$ age of 123±1 Ma (MSWD=1.2) (Fig. 6g). Sample FW04-409 is a porphyritic rhyolite with a felsitic matrix. The phenocrysts are mainly sanidine, biotite and quartz. All the data spots plot on or near concordia (Fig. 6h) and thirteen analyses yield a $^{206}Pb/^{238}U$ weighted mean age of 118±2 Ma (MSWD=8.2). Samples FW04-418 and FW04-419 are both dacite, with a porphyritic texture defined by rare phenocrysts of plagioclase, set in a felsitic matrix. Data for sample FW04-418 mainly plot to the right of the concordia curve (Fig. 6i), which may be the result of an inappropriate common lead correction, since high common lead is suggested by the dark CL images. Eighteen analyses of zircon from this sample yield a weighted mean $^{206}Pb/^{238}U$ age of 113±2 Ma (MSWD=10.9, Fig. 6i), and 22 analyses of zircons from sample FW04-419 give a weighted mean $^{206}Pb/^{238}U$ age of 116±a (MSWD=2.6) (Fig. 6j).

5.3. Yiliekede Formation

The Yiliekede Formation is the uppermost unit in the Mesozoic volcanic sequence in the Great Xing'an Range,

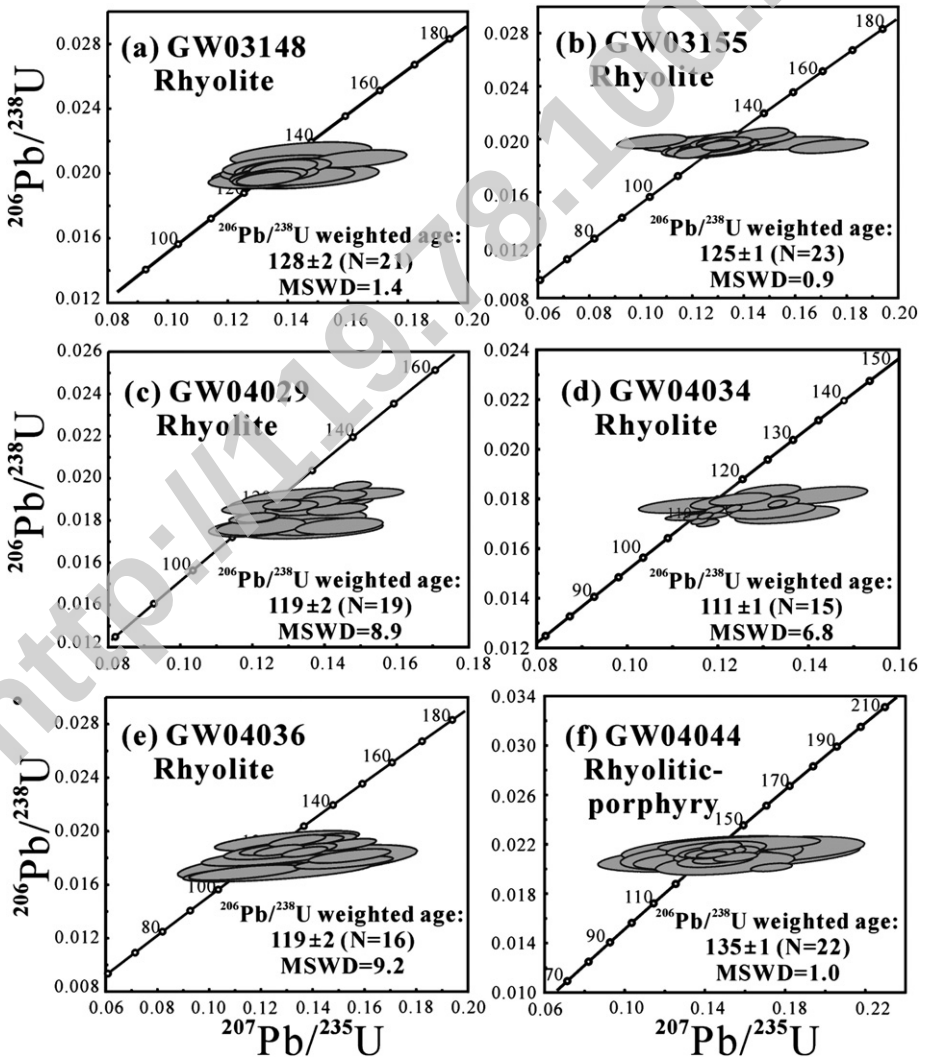

Fig. 6. U–Pb concordia diagrams of zircon data from felsic volcanic rocks of the Shangkuli Formation (LA-ICPMS analyses). (a) sample GW03148, (b) sample GW03155, (c) sample GW04029, (d) sample GW04034, (e) sample GW04036, (f) sample GW04044, (g) sample FW04-401, (h) sample FW04-409, (i) sample FW04-418, (j) sample FW04-419.

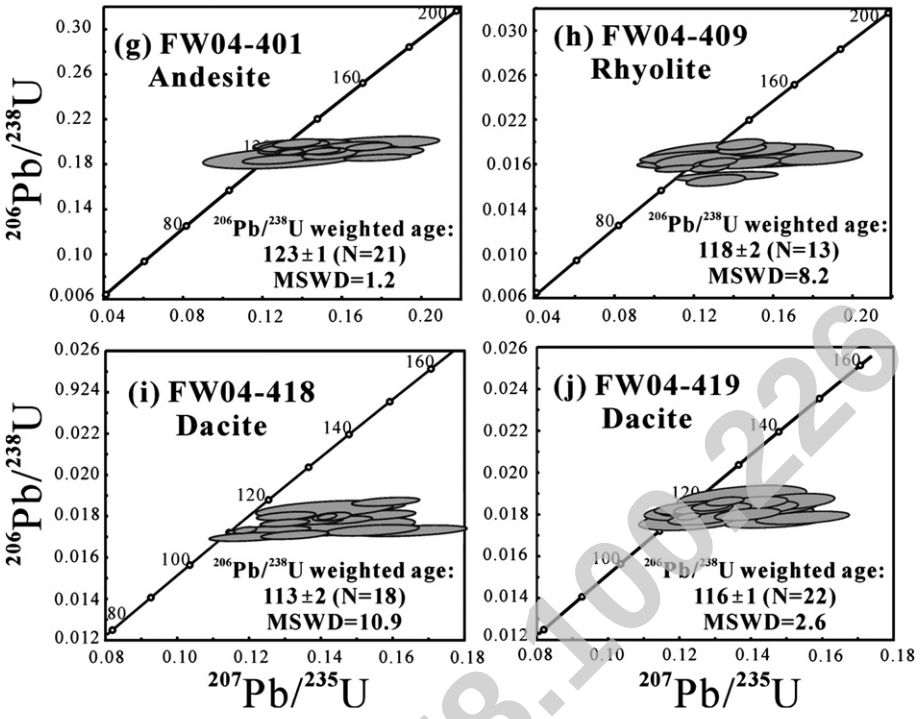

Fig. 6 (*continued*).

so its eruption age will provide important constraints on the termination of volcanism in the region. In this study, two basalts containing zircons were dated by LA-ICPMS (samples FW04-420 and GW03120) and two by whole rock $^{40}Ar/^{39}Ar$ method (samples GW04027 and GW04032).

Sample FW04-420 is an andesite collected from the eastern Great Xing'an Range. Although the analyses show a complex age pattern, 6 analyses of magmatic zircons with oscillatory zoning yield a weighted mean $^{206}Pb/^{238}U$ age of 123±2 Ma (MSWD=1.2, Fig. 7a), which are taken to represent the eruption age of the rock. The other analyses include Archean $^{207}Pb/^{206}Pb$ ages (Fig. 7a) and are considered to be recording inherited zircon, indicating that Archean material is present in the basement of the region. Zircons in basalt sample GW03120 from the northern part of the area also show a complicated pattern of ages and three populations can be identified. Six analyses of magmatic zircon (Fig. 4m) yield a weighted mean $^{206}Pb/^{238}U$ age of 126±5 Ma (MSWD=3.9, Fig. 7b) and are taken to represent the age of basaltic eruption. Zircons of the second and third groups display distinctive oscillatory zoning in CL images, and give weighted mean $^{206}Pb/^{238}U$ ages of 481±5 (n=8, MSWD=1.0) and 779±10 Ma (n=3, MSWD=0.1) (Fig. 7b), consistent with the timing of Early Paleozoic and Neoproterozoic granites in the region (Ge et al., 2005a). These zircons were thus inherited from the basement.

Two fine-grained basalts from the Yiliekede Formation (GW04027 and GW04032) were dated using the whole rock $^{40}Ar/^{39}Ar$ incremental heating technique, since not enough zircons were present for meaningful U–Pb analysis. Seven steps from sample GW04032 yield an inverse isochron age of 117.5±1.3 Ma and an initial $^{40}Ar/^{36}Ar$ of 313±51 (MSWD=1.4) (Fig. 7c). The first 5 steps were excluded in the age calculation because of the large deviation from the inverse isochron line, which may be caused by the absorption of surficial ^{40}Ar. The same data define a plateau age of 117.6±1.2 Ma (Fig. 7d), which is identical to the inverse isochron age. Sample GW04027 came from the locality where the Yiliekede Formation was first defined. The analyses display homogeneous Ar isotopic compositions. Ten steps of data define an inverse isochron with an age of 112.2±2.1 Ma (MSWD=7.9) (Fig. 7e). The initial $^{40}Ar/^{36}Ar$ defined by the isochron line is 301±46, which is equal to the atmospheric value within error, indicating no excess Ar was trapped. The plateau age defined by these steps is 112.4±1.3 Ma (Fig. 7f), consistent with the isochron age. Therefore, 112.2±2.1 Ma is considered as the eruption age of the rock.

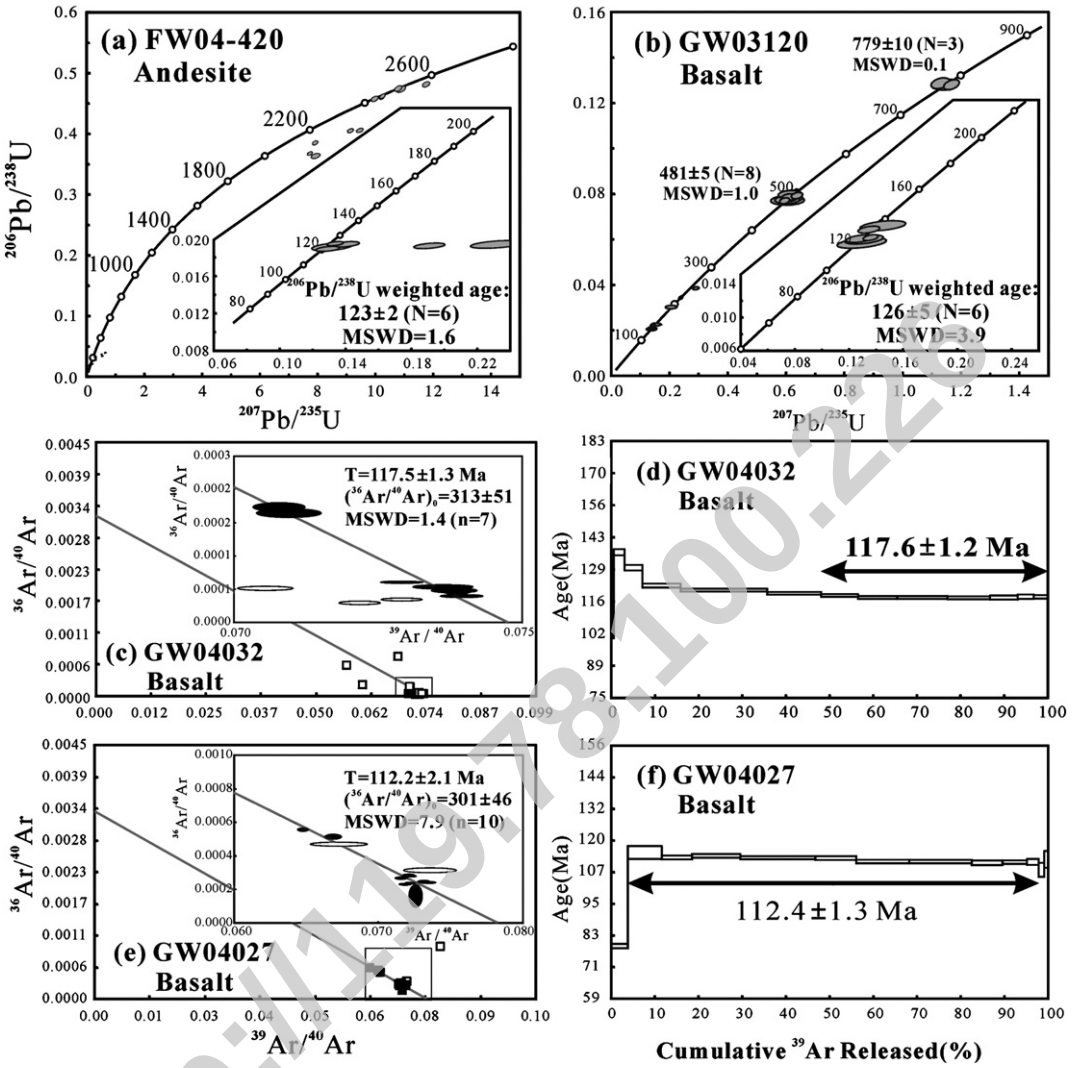

Fig. 7. Geochronological diagrams of the Yiliekede basalts and andesite. (a) sample FW04-420 (zircon laser U–Pb), (b) sample GW03120 (zircon laser U–Pb), (c) and (d) sample GW04032 (whole-rock Ar–Ar), (e) and (f) sample GW04027 (whole-rock Ar–Ar).

5.4. Related dykes

In the Great Xing'an Range, a large number of mafic to felsic dykes are present. In the central part of the Great Xing'an Range, the dykes intrude into Paleozoic granite and show obvious evidence of magma mixing (Zhang et al., 2006). Zircon LA-ICPMS U–Pb analyses of a coarse-grained dolerite (sample GW04005, Fig. 4n) yield a weighted mean $^{206}Pb/^{238}U$ age of 124±2 Ma, whereas a porphyry (sample 9411-A) has a weighted mean $^{206}Pb/^{238}U$ age of 130±1 Ma (Fig. 8a and b). Another dolerite (sample GW03285) from the northernmost part of the Great Xing'an Range has a complicated age pattern. Four analyses yield a weighted mean $^{206}Pb/^{238}U$ age of 133±3 Ma (MSWD=1.2) (Fig. 8c), which is considered as the emplacement age of the dyke. However, most of zircons show Neoproterozoic ages, indicating inheritance from older basement.

6. Discussion

6.1. Eruption ages of the Mesozoic volcanic rocks in the Great Xing'an Range

It was previously suggested that the Mesozoic volcanic rocks in the Great Xing'an Range were erupted during the Middle Jurassic to Early Cretaceous (IMBGMR, 1991; HBGMR, 1993; Wang et al., 1997). Combined with

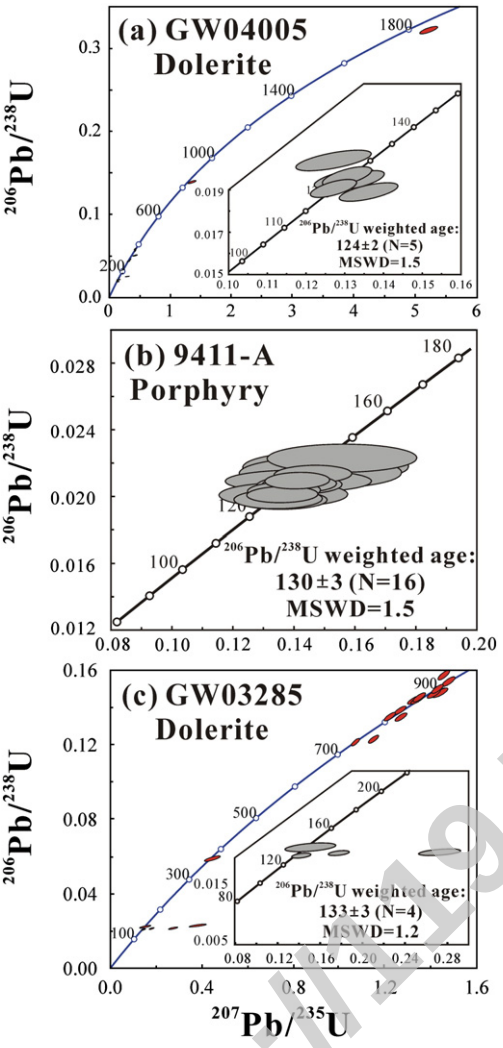

Fig. 8. U–Pb concordia diagrams of zircon data from mafic/felsic dykes in the Great Xing'an Range (LA-ICPMS analyses). (a) sample GW04005 (dolerite), (b) sample 9411-A (porphyry) and (c) sample GW03285 (dolerite).

recently reported data, it is possible for us to evaluate the proposed chronological scheme, since a new set of twenty-seven ages has been obtained in this study. Although the Tamulangou Formation was previously considered to have formed in the Middle-Late Jurassic, our data do not support this conclusion, since the ages show a large range from 186.3±2.8 to 128±8 Ma. Wu et al. (2005b) dated a basalt from this formation and obtained an $^{40}Ar/^{39}Ar$ age of 122.2±2.7 Ma. Wang et al. (2006) conducted a comprehensive study of this formation using the whole rock $^{40}Ar/^{39}Ar$ dating method, and the ages ranged from 160.0±0.9 to 140.7±1.1 Ma, reasonably consistent with our new results. Therefore, it is concluded that the Tamulangou Formation was erupted over a long time span from 186 to 121 Ma (Fig. 9a). In detail, this formation can be divided into 4 individual eruption stages, i.e., at ~180 Ma, 165–160 Ma, 150–140 Ma and 125 Ma. If we accept the proposed stratigraphic column shown by Fig. 2, some of the so-called Tamulangou rocks may belong to the Shangkuli and Yilikede formations as discussed below, and should not in future be considered as Tamulangou Formation.

The Shangkuli Formation was considered to have been formed during the Late-Jurassic to Early Cretaceous (HBGMR, 1993). However, the Rb–Sr isochron age of 127±5 Ma reported by Ge et al. (2001) indicated its eruption probably took place in the Early Cretaceous. Recently, Wang et al. (2006) published eight ages of basalts from this formation, obtaining ages ranging from 124.7 ±0.7 Ma to 120.7±1.3 Ma, also indicating their eruption in the Early Cretaceous. Considering that the volcanic rocks of this formation occupy a significant area in the northern Great Xing'an Range and are characterized by the occurrence of rhyolite and dacite, we concentrated our dating on these felsic rocks. Our ten ages indicate that the eruption of the Shangkuli Formation took place between 135±1 Ma and 111±1 Ma, with most activity between 130-120 Ma. Therefore, the Shangkuli Formation has a narrower eruption age range than the Tamulangou Formation (Fig. 9b) and is entirely of Cretaceous age.

The Yiliekede Formation, the uppermost unit of the volcanic sequence in the Great Xing'an Range, was previously considered to have formed during the Early Cretaceous. However, reliable ages were lacking until recently. Using the $^{40}Ar/^{39}Ar$ whole-rock method, Wu et al. (2005b) obtained an age of 116.7±2.5 Ma for a basalt, whereas five ages reported by Wang et al. (2006) using the same method, range from 116.0±0.8 to 106.1±1.1 Ma. In our study, four samples yielded ages ranging from 126±5 Ma to 112.2±2.1 Ma, consistent with previously reported data. Therefore, it is concluded that the Yiliekede Formation was erupted between 126–106 Ma in the Early Cretaceous, with peak activity at ~115 Ma (Fig. 9c).

Based on these new precise age data, a four stage geochronological framework for the volcanic rocks in the Great Xing'an Range can be established, i.e., events at ~180 Ma, 165–160 Ma, 150–135 Ma and 130–105 Ma (Fig. 9d). The first three stages of volcanic activity are represented by the Tamulangou rocks, and the last stage is represented by the Shangkuli and Yiliekede formations. It is clear from this scheme that, in terms of volume, the volcanic rocks in the area were mainly erupted during the last stage with an age range of 130–110 Ma and a peak at 125 Ma. Therefore, the Early

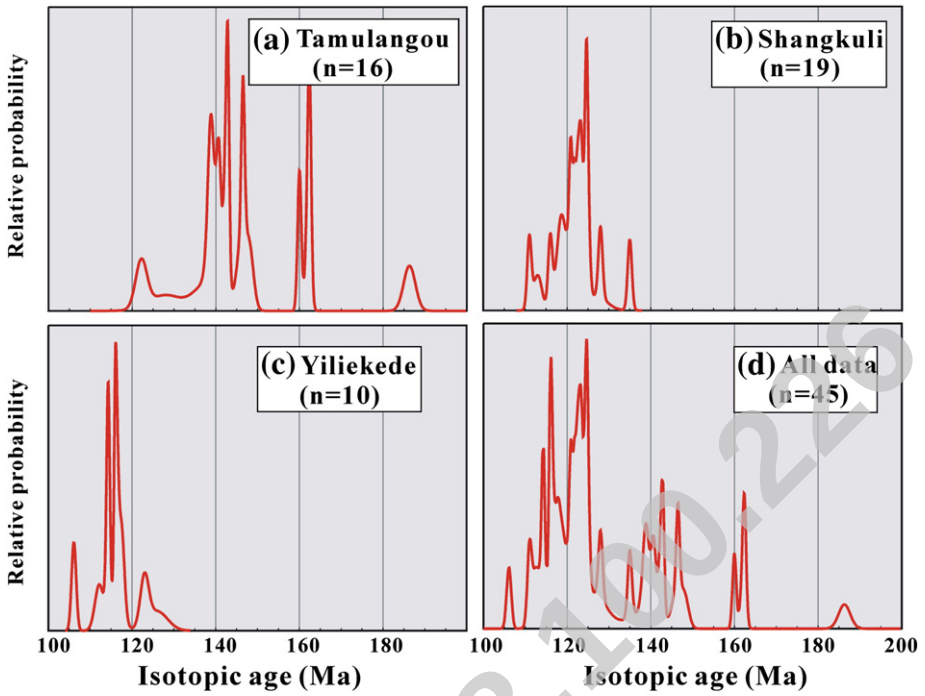

Fig. 9. Probability diagrams for the volcanic rocks in the Great Xing'an Range. (a) Tamulangou Formation (16 ages), (b) Shangkuli Formation (19 ages), (c) Yiliekede Formation (10 ages), and (d) all the data (45 ages) (Data sources: Wu G. et al., 2005c,d; Wang et al., 2006 and this study).

Cretaceous was the major period of Mesozoic volcanism in the Great Xing'an Range.

Our new data challenge the conventional stratigraphic subdivision and regional correlation of the volcano-sedimentary strata in the Great Xing'an Range. Firstly, basalts are normally classified as Tamulangou Formation when overlain by rhyolite, or as Yiliekede Formation where they overlie rhyolite–dacite (Fig. 2). However, the basalts are also interlain with rhyolite in the Shangkuli Formation, and therefore the distinctions between basalts in the Tamulangou, Shangkuli and the Yiliekede formations are vague in terms of field occurrence, petrography and geochemistry, which make this scheme inapplicable. Secondly, as shown in Fig. 9, there is some overlap in age between the Tamulangou, Shangkuli and Yiliekede formations. Therefore, the stratigraphic sequence of the Mesozoic volcanic rocks in some parts of this region needs to be re-evaluated according to the new precise geochronological data. This is especially true for the Tamulangou Formation in areas where it is not covered directly by rhyolite, since the basalt here might belong to the Yiliekede or Shangkuli formations. Considering all the presently available data, we suggest that the terms Tamulangou, Shangkuli and Yiliekede be considered as "episodes" and used to cover the rocks formed in three separate stages at 185–135, 135–120 and 120–105 Ma, respectively.

6.2. Tectonic setting of Mesozoic volcanism in the Great Xing'an Range

Several schemes have been proposed to interpret the tectonic setting in which the Mesozoic volcanic rocks in the Great Xing'an Range formed. Based on the supposed circular distribution of Mesozoic volcanic rocks within and around the Great Xing'an Range, it was proposed that a mantle plume or some similar intraplate process might be responsible for the formation of such a huge area of volcanic rocks (Shao et al., 1994, 2001a,b; Lin et al., 1998; Deng et al., 1996; Ge et al., 1999). However, the linear distribution of the Mesozoic volcanic rocks along the whole of the Great Xing'an Range, and even extending into eastern China, does not support this interpretation (Fig. 1a). Moreover, as seen from the data set, magmatic activities extended from 185 to 105 Ma, much longer than the period normally associated with a mantle plume. Therefore, we do not consider that a mantle plume is responsible for the generation of the Mesozoic volcanic rocks in the Great Xing'an Range.

The second model suggests that the Mesozoic volcanic rocks were formed due to subduction of the Mongol–Okhotsk Ocean and subsequent orogenic collapse (Fan et al., 2003; Guo et al., 2001; Wang et al., 2002; Meng, 2003). Although it might be argued that the Jurassic basalt, exposed in the western part of the Great Xing'an Range,

might be related to subduction and closure of the Mongol–Okhotsk Ocean, the following lines of evidence do not support this interpretation. According to the available seismic tomography (Van der Voo et al., 1999), the Mongol–Okhotsk Ocean subducted northward beneath Siberia, not southward beneath the Great Xing'an Range as required in the model. This means that the Mesozoic volcanic rocks in the Great Xing'an Range could not be formed by subduction of the Mongol–Okhotsk Ocean since these rocks are distributed not only in the Great Xing'an Range of China, but also in eastern Mongolia and in Russia. Also, if rocks in the Great Xing'an Range were considered as the product of post-orogenic evolution after suturing prior to ~170 Ma (Tomurtogoo et al., 2005), it is difficult to explain why these rocks extend in a NNE direction, not in a NE direction parallel to the Mongol–Okhotsk Ocean suture (Fig. 1 of Meng (2003)). Moreover, as we will discuss below, coeval Mesozoic volcanic rocks are widely distributed in the main continental area of eastern China, which cannot be explained by the collapse of the Mongol–Okhotsk orogen.

The third model that has been proposed involves subduction of the Paleo-Pacific plate beneath eastern China (Uyeda and Miyashiro, 1974; Hilde et al., 1977; Jiang and Quan, 1988; Zhao et al., 1989; Sengör and Natal'in, 1996; Wang et al., 2006). There are several lines of evidence that support this interpretation. Firstly, the Mesozoic volcanic rocks in NE China and surrounding areas are distributed in a NNE direction (Fig. 1a), parallel to the NNE-oriented Asian continental margin. Secondly, geophysical data indicate that there is a high velocity zone beneath eastern China (Fukao et al., 1992; Huang and Zhao, 2006), which is commonly considered to be the result of a megalith of subducted oceanic crust. Thirdly, it has been documented that Jurassic–Cretaceous accretionary complexes are extensively developed along the whole of the Asian continental margin (Kojima, 1987; Natal'in, 1993; Isozaki, 1997; Maruyama, 1997; Wu et al., 2007a,b), undoubtedly indicating a subduction regime related to the Paleo-Pacific plate.

Therefore, the Mesozoic volcanic rocks in the Great Xing'an Range appear most likely related to subduction of the Paleo-Pacific plate. However, some older components, exposed in the western part with ages between 186 to 160 Ma, might be related to closure of the Mongol–Okhotsk Ocean, but more data are required to verify this.

6.3. Geodynamic model for large-scale Early Cretaceous magmatism in the Great Xing'an Range

Although we favour a causal link between subduction of the Paleo-Pacific plate and the formation of the Mesozoic volcanic rocks in the Great Xing'an Range, it is still unclear whether or not these rocks were formed by partial melting of the mantle wedge which was metasomatized by fluid dehydrated from the subducted oceanic crust. Based on the spatial–temporal variations, Wang et al. (2006) proposed a migrating delamination model for the lithosphere above the subduction zone, although the data they cited are incomplete. For example, Jurassic magmatic rocks are also widely distributed to the east of the Great Xing'an Range, in the Zhangguangcai Range (Wu et al., 2007a), Liaodong Peninsula (Wu et al., 2005b) and Korean Peninsula (Sagong and Kwon, 2005; Wu et al., 2007b). Therefore, the model requires more data to verify it.

However, it is clear from the available age data that Mesozoic volcanism in the northern Great Xing'an Range mostly took place in the Early Cretaceous, with a peak at 125 Ma. Although we only report age results from the northern Great Xing'an Range, dating of volcanic rocks from the southern part of the range also yields similar Early Cretaceous ages (Zhang, 2006). Early Cretaceous volcanic rocks are also widespread in other areas of NE China and Mongolia (Smith et al., 1995; Swisher et al., 1999, 2002; Davis et al., 2001; Graham et al., 2001; Wang et al., 2001a, 2001b, 2002; Chen, 2003; Peng et al., 2003; Pei et al., 2005). Similarly, igneous rocks of this age are also widespread in other region of eastern China, including the eastern NCC, in the Dabie–Sulu ultrahigh pressure belt and in the eastern Yangtze Craton of southeastern China. Therefore, the Early Cretaceous was the most important period of magmatism in NE China and surrounding areas and the Great Xing'an Range is an important component of the Early Cretaceous giant igneous province in Eastern China as defined by Wu et al. (2005a,b).

The question remains as to what caused this giant Early Cretaceous igneous event in NE China. Although it is still controversial, many researchers have noticed that the volcanic rocks, as well as other types of igneous rocks, were generated in an extensional environment (Ge et al., 2001; Guo et al., 2001; Shao et al., 2001a,b; Fan et al., 2003; Lin et al., 2003; Gao et al., 2005; Wu et al., 2005a,b). The following lines of evidence support this conclusion. Firstly, a large number of A-type granites and other alkaline rocks, coeval with the volcanic rocks reported in this study, have been identified in the Great Xing'an Range (Li and Yu, 1993; Wang and Zhao, 1997; Ge et al., 2001; Jahn et al., 2001; Lin et al., 2003; Wu et al., 2002; Ge et al., 2005b). Similar A-type granites and alkali rocks are also widely distributed throughout eastern China (Wu et al., 2005a,b). Secondly, an extensional environment is also indicated by the development of metamorphic core complexes (MCC)

in the region (Yang et al., 1996; Zhang et al., 1998; Liu et al., 2005), including the occurrence of the Ganzhuermiao MCC in the Great Xing'an Range reported by Zhang et al. (1998). Although the exact age of this MCC has not been precisely determined, the rock association indicates that it is contemporaneously with Mesozoic volcanism (Zhang et al., 1998). Zhang et al. (2000) reported another MCC in the Songliao Basin, where Ar–Ar dating of a mylonite yields an age of 126.7±1.5 Ma, coeval with the giant igneous event identified by Wu et al. (2005a,b). Thirdly, the wide occurrence of coeval mafic–felsic dykes in the Great Xing'an Range and nearby areas is also an important line of evidence of an extensional setting during the Early Cretaceous (Shao et al., 1998, 2001a,b; Shao and Zhang, 2002; Zhang et al., 2006).

The question remains as to what can cause such a large-scale igneous event in an extensional setting. Since it has recently been established that the Early Cretaceous was the time of lithospheric thinning in the eastern NCC (Wu et al., 2005a,b), resulting in the removal of >100 km of lithosphere (Menzies et al., 1993; Menzies and Xu, 1998; Griffin et al., 1998; Wu and Sun, 1999, Wu et al., 2000a, 2003a,b, 2006; Xu, 2001; Gao et al., 2002, 2004; Zhang, 2005; Zheng et al., 2006) and accompanied by large scale magmatism at 125 Ma, we therefore propose that lithospheric thinning is also likely to be the main causing of volcanism in the Great Xing'an Range in the Early Cretaceous. Based on the above analysis, we propose that Jurassic subduction of the Paleo-Pacific plate resulted in lithospheric thickening in eastern China, extending from coastal NE China in the north, across the NCC in the central part to SE China in the south. The dehydration of subducted oceanic crust would soften the previously thickened lithosphere, and result in delamination due to gravitational instability; and the subsequent upwelling of new asthenospheric mantle, which triggered voluminous magmatism across all of eastern China in the Early Cretaceous. We thus propose that lithospheric thinning took place throughout NE China, and was not limited to the NCC.

7. Conclusions

A comprehensive zircon U–Pb and whole-rock Ar–Ar dating program in the Great Xing'an Range has led to the following conclusions:

1) The Mesozoic volcanic rocks in the Great Xing'an Range were erupted from the Early Jurassic to the Early Cretaceous, but the main activity took place during the Early Cretaceous, with a peak at 125 Ma. This forms an important component of the Early Cretaceous giant igneous event in eastern China;
2) The new precise age data indicate that the previous stratigraphic sub-divisions of the Mesozoic volcanic rocks in the Great Xing'an Range need to be re-evaluated, since the data do not support the traditional stratigraphic interpretation;
3) The occurrence of A-type rocks in the Great Xing'an Range implies that the associated Early Cretaceous volcanic rocks were generated in an extensional environment. The similarities in rock type and age to components of the NCC indicate that the immense eruption of Mesozoic volcanic rocks in the Great Xing'an Range may have a close relationship to subduction of the Pacific plate, which some have suggested also triggered lithospheric thinning beneath the whole of eastern China, thus resulting in a giant igneous event in the Late Mesozoic.

Acknowledgements

We are grateful to Shan Gao, Hong-Lin Yuan and Chun-Rong Diwu at the State Key Laboratory of Continental Dynamics (Northwest University), Ministry of Education, as well as Yu-Guang Ma and Mao Qian at the Institute of Geology and Geophysics, Chinese Academy of Sciences, for their help with analyses. We are grateful to R. Rudnick, B. M. Jahn, B. Natal'in, as well as an anonymous reviewer, for their constructive comments on the manuscript. This work was financially supported by the National Natural Science Foundation of China (Grants 40325006, 40421202 and 40372038) and a Special Grant of Oil & Gas Research (XQ-2004-07).

Appendix A. Supplementary data

Supplementary data associated with this article can be found, in the online version, at doi:10.1016/j.lithos.2007.08.011.

References

Andersen, T., 2003. Correction of common lead in U–Pb analyses that do not report ^{204}Pb. Chem. Geol. 192, 59–79.

Ballard, J.R., Palin, J.M., Williams, I.S., Campbell, I.H., Faunes, A., 2001. Two ages of porphyry intrusion resolved for the super-giant Chuquicamata copper deposit of northern Chile by ELA-ICP-MS and SHRIMP. Geology 29, 383–386.

Black, L.P., Kamo, S.L., Allen, C.M., Davis, D.W., Aleinikoff, J.N., Wallay, J.W., Mundil, R., Campbell, I.H., Korsch, R.J., Williams, I.S., Foudoulis, C., 2004. Improved ^{206}Pb/^{238}U microprobe geochronology by the monitoring of a trace-element-related matrix effect: SHRIMP, ID-TIMS, ELA-ICP-MS and oxygen isotope documentation for a series of zircon standards. Chem. Geol. 206, 115–140.

Chen, Y.J., 2003. Stratigraphic studies on the Mesozoic volcanism in the southeastern Jilin Province. Doctoral Dissertation, Jilin University, 1−105.

Chen, B., Jahn, B.M., Wilde, S., Xu, B., 2000. Two contrasting Paleozoic magmatic belts in northern Inner Mongolia, China: petrogenesis and tectonic implications. Tectonophysics 328, 157–182.

Davis, G.A., Zheng, Y.D., Wang, C., Darby, B.J., Zhang, C.H., Gehrels, G., 2001. Mesozoic tectonic evolution of the Yanshan fold and thrust belt, with emphasis on Hebei and Liaoning Provinces, northern China. In: Hendrix, M.S., Davies, G.A. (Eds.), Paleozoic and Mesozoic tectonic evolution of central Asia: From continental assembly to intracontinental deformation: GSA Memoir, 194, pp. 171–198.

Deng, J.F., Zhao, H.L., Mo, X.X., Luo, Z.H., Du, S.Y., 1996. Continental root/plume structure in China-key to the continental geodynamics. Geological Publishing House, Beijing, pp. 1–110.

Fan, W.M., Guo, F., Wang, Y.J., Lin, G., 2003. Late Mesozoic calc-alkaline volcanism of post-orogenic extension in the northern Da Hinggan Mountains, Northeastern China. J. Volcano. Geotherm. Res. 121, 115–135.

Flisch, M., 1982. Potassium-argon analysis. In: Odin, G.S. (Ed.), Numerical dating in stratigraphy. Wiley, Chichester, pp. 151–158.

Fukao, Y., Obayashi, M., Inoue, H., Nenbai, M., 1992. Subducting slabs stagnant in the mantle transition zone. J. Geophys. Res. 97, 4809–4822.

Gao, S., Rudnick, R.L., Carlson, R.W., McDonough, W.F., Liu, Y.S., 2002. Re–Os evidence for replacement of ancient mantle lithosphere beneath the North China Craton. Earth Planet. Sci. Lett. 198, 307–322.

Gao, S., Rudnick, R.L., Yuan, H.L., Liu, X.M., Liu, Y.S., Xu, W.L., Ling, W.L., Ayers, J., Wang, X.C., Wang, Q.H., 2004. Recycling lower continental crust in the North China Craton. Nature 432, 892–897.

Gao, X.F., Guo, F., Fan, W.M., Li, C.W., Li, X.Y., 2005. Origin of Late Mesozoic intermediate-felsic volcanic rocks from the northern Da Hinggan Mountain, NE China. Acta Petrol. Sinica 21, 737–748 (in Chinese with English abstract).

Ge, W.C., Lin, Q., Sun, D.Y., Wu, F.Y., Won, C.K., Lee, M.W., Jin, M.S., Yun, S.H., 1999. Geochemical characteristics of the Mesozoic basalts in Da Hinggan Ling: evidence of the mantle-crust interaction. Acta Petrol. Sinica 15, 397–407 (in Chinese with English abstract).

Ge, W.C., Lin, Q., Sun, D.Y., Wu, F.Y., Li, X.H., 2000. Geochemical research into origins of two types of Mesozoic rhyolites in Da Xing'an Ling. Earth Sci. 25, 172–178 (in Chinese with English abstract).

Ge, W.C., Li, X.H., Lin, Q., Sun, D.Y., Wu, F.Y., Yun, S.H., 2001. Geochemistry of early Cretaceous alkaline rhyolites from Hulun Lake, Da Xing'an Ling and its tectonic implication. Chinese J. Geol. 36, 176–183 (in Chinese with English abstract).

Ge, W.C., Wu, F.Y., Zhou, C.Y., Abdel Rahman, A.A., 2005a. Emplacement age of the Tahe granite and its constraints on the tectonic nature of the Erguna block in the northern part of the Great Xing'an Range. Chin. Sci Bull. 50, 2097–2105.

Ge, W.C., Wu, F.Y., Zhou, C.Y., Zhang, J.H., 2005b. Zircon U–Pb ages and its significance of the Mesozoic granites in the Wulanhaote Region, central Great Xing'an Range. Acta Petrol. Sinica 21, 749–762 (in Chinese with English abstract).

Guo, F., Fan, W.M., Wang, Y.J., Lin, G., 2001. Petrogenesis of the late Mesozoic bimodal volcanic rocks in the southern Da Hinggan Mts., China. Acta Petrol. Sinica 17, 161–168 (in Chinese with English abstract).

Graham, S.A., Hendrix, M.S., Johnson, C.L., Badamgarav, D., Badarch, G., Amory, J., Porter, M., Barsbold, R., Webb, L.E., Hacker, B.R., 2001. Sedimentary record and tectonic implications of Mesozoic rifting in southeast Mongolia. Geol. Soc. Amer. Bull. 113, 1560–1579.

Griffin, L.L., Zhang, A.D., O'Reilly, S.Y., Ryan, C.G., 1998. Phanerozoic evolution of the lithosphere beneath the Sino-Korean craton. In: Flower, M.F.J., Chung, S.L., Lo, C.H., Lee, T.Y. (Eds.), Mantle Dynamics and Plate Interactions in East Asia. Am. Geophy. Union, Washington, D.C., Geodyn. Ser., vol. 100, pp. 107–126.

Harris, A.C., Allen, C.M., Bryan, S.E., Campbell, I.H., Holcombe, R.J., Palin, J.M., 2004. ELA-ICP-MS U–Pb zircon geochronology of regional volcanism hosting the Bajo de la ALumbrera Cu–Au deposit: implication for porphyry-related mineralization. Min. Dep. 39, 46–67.

HBGMR (Heilongjiang Bureau of Geology and Mineral Resources), 1993. Regional geology of Heilongjiang Province. Geological Publishing House, Beijing, pp. 1–734 (in Chinese with English abstract).

Hilde, T.W.C., Uyeda, S., Kroenke, L., 1977. Evolution of the western Pacific and its margin. Tectonophysics 38, 145–165.

Hong, D.W., Huang, H.Z., Xiao, Y.J., Xu, H.M., Jin, M.Y., 1994. The Permian alkaline granites in central Inner Mongolia and the geodynamic significance. Acta Geol. Sinica (Chinese edtion) 68, 219–230 (in Chinese with English abstract).

Huang, J.L., Zhao, D.P., 2006. High-resolution mantle tomography of China and Surrounding regions. J. Geophy. Res. 111, B09305. doi:10.1029/2005JB004066.

(IMBGMR) Inner Mongolia Bureau of Geology and Mineral Resources, 1991. Regional Geology of Inner Mongolia. Geological Publishing House, Beijing, pp. 1–725 (in Chinese with English abstract).

Irvine, T.N., Baragar, W.R.A., 1971. A guide to the chemical classification of the common volcanic rocks. Can. J. Earth Sci. 8, 523–548.

Isozaki, Y., 1997. Jurassic accretion tectonics of Japan. Island Arc 6, 25–51.

Jackson, S.E., Pearson, N.J., Griffin, W.L., Belousova, E.A., 2004. The application of laser ablation-inductively coupled plasma-mass spectrometry (LA-ICP-MS) to in-situ U–Pb zircon geochronology. Chem. Geol. 211, 331–335.

Jahn, B.M., Wu, F.Y., Chen, B., 2000. Massive granitoid generation in central Asia: Nd isotopic evidence and implication for continental growth in the Phanerozoic. Episodes 23, 82–92.

Jahn, B.M., Wu, F.Y., Capdevila, R., Martineau, F., Zhao, Z.H., Wang, Y.X., 2001. Highly evolved juvenile granites with tetrad REE patterns: the Woduhe and Baerzhe granites from the Great Xing'an Mountains in NE China. Lithos 59, 171–198.

Jiang, G.Y., Quan, H., 1988. Mesozoic volcanic rocks of Genhe and Hailar basins in Da Hinggan Ling Range. Bull. Shenyang Inst. Res., Chinese Acad. Geol. Sci. 17, 23–100 (in Chinese with English abstract).

Kojima, S., 1987. Mesozoic terrane accretion in northeast China, Sikhote-Alin and Japan regions. Palaeogeogr. Palaeoclimatol. Palaeoecol. 69, 213–232.

Li, R.S., 1991. Xinlin ophiolite. Heilongjiang Geol. 2, 19–32 (in Chinese with English abstract).

Li, P.Z., Yu, J.S., 1993. Nianzishan miarolitic alkaline granite stock, Heilongjiang-its age and geological implications. Geochimica 4, 389–398 (in Chinese with English abstract).

Li, H.M., Dong, C.W., Xu, X.S., Zhou, X.M., 1995. The single grain zircon U–Pb age of the Quanzhou gabbro-the source of mafic

igneous rock in Southeast Fujian Province. Chin. Sci. Bull. 40, 158–160 (in Chinese).

Li, X.H., Liang, X.R., Sun, M., Guan, H., Malpas, J.G., 2001. Precise $^{206}Pb/^{238}U$ age determination on zircons by laser ablation microprobe-inductively coupled plasma-mass spectrometry using continuous linear ablation. Chem. Geol. 175, 209–219.

Liang, X.R., Li, X.H., Liu, Y.K., Zhu, B.Q., Zhang, H.Y., 2000. U–Pb isotopic of young zircons by laser ablation microprobe-inductively coupled plasma mass spectrometry (LAM-ICPMS). Geochimica 29, 1–5 (in Chinese with English abstract).

Lin, Q., Ge, W.C., Sun, D.Y., Wu, F.Y., Won, C.K., Min, K.D., Jin, M.S., Lee, M.W., Kwon, C.S., Yun, S.H., 1998. Tectonic implications of Mesozoic volcanic rocks in Northeastern China. Sci. Geol. Sin. 33, 129–139 (in Chinese with English abstract).

Lin, Q., Ge, W.C., Sun, D.Y., Wu, F.Y., Won, C.K., Lee, M.W., Yun, S.H., Jin, M.S., Min, K.D., Kwon, C.S., 2000. Genetic relationships between two types of Mesozoic rhyolites and basalts in Great Xing'an Ridge. J. Changchun Uni. Sci. Tech. 30, 322–328 (in Chinese with English abstract).

Lin, Q., Ge, W.C., Cao, L., Sun, D.Y., Lim, K.G., 2003. Geochemistry of Mesozoic volcanic rocks in Da Hinggan Ling: the bimodal volcanic rocks. Geochimica 32, 208–222 (in Chinese with English abstract).

Lin, Q., Ge, W.C., Wu, F.Y., Sun, D.Y., Cao, L., 2004. Geochemistry of Mesozoic granites in Da Hinggan Ling ranges. Acta Petrol. Sinica 20, 403–412 (in Chinese with English abstract).

Liu, H.C., Zhu, B.Q., Zhang, Z.X., 1998. Single zircon dating by LAM-ICPMS technique. Chin. Sci. Bull. 43, 1103–1106 (in Chinese).

Liu, J.L., Davis, G.A., Lin, Z.Y., Wu, F.Y., 2005. The Liaonan metamorphic core complex, Southeastern Liaoning Province, North China: a likely contributor to Cretaceous rotation of Eastern Liaoning, Korea and contiguous areas. Tectonophysics 407, 65–80.

Ludwig, K.R., 2003. Isoplot 3.0 — a geochronological toolkit for Microsoft Excel. Berkeley Geochronology Center, Spec. Publ., vol. 4. 70 pp.

Maruyama, S., 1997. Pacific-type orogeny revisited: Miyashiro-type orogeny proposed. The Island Arc 6, 91–120.

Meng, Q.R., 2003. What drove late Mesozoic extension of the northern China–Mongolia tract? Tectonophysics 369, 155–174.

Menzies, M.A., Fan, W.M., Zhang, M., 1993. Paleozoic and Cenozoic lithospheres and the loss of >120km of Archean lithosphere, Sino-Korean craton, China. In: Prichard, H.M., Alabaster, T., Harris, N.B.W., Neary, C.R. (Eds.), Magmatic Processes and Plate Tectonics. Spec. Publ. Geol. Soc. London., vol. 76, pp. 71–81.

Menzies, M.A., Xu, Y.G., 1998. Geodynamics of the North China craton. In: Flower, M.F.J., Chung, S.L., Lo, C.H., Lee, T.Y. (Eds.), Mantle Dynamics and Plate Interactions in East Asia. Am. Geophy. Union, Washington, D.C., Geodyn. Ser., vol. 100, pp. 155–165.

Miao, L.C., Fan, W.M., Zhang, F.Q., Liu, D.Y., Jian, P., Shi, G.H., Tao, H., Shi, Y.R., 2004. SHRIMP zircon geochronology of the Xinkailing–Kele complex in the northwestern Lesser Xing'an Range, and its geological implications. Chin. Sci. Bull. 49, 201–209.

Natal'in, B.A., 1993. History and modes of Mesozoic accretion in southeastern Russia. Island Arc 2, 15–34.

Pei, F.P., Xu, W.L., Yang, D.B., Ji, W.Q., Gao, F.H., 2005. The forming time of the Mesozoic volcanic rocks in the south Songliao basin and constraints on the characteristics of the basement. Abstract of 2005 National Petrology and Geodynamics Meeting, p. 108 (in Chinese).

Peng, Y.D., Zhang, L.D., Chen, W., Zhang, C.J., Guo, S.Z., Xing, D.H., Jia, B., Chen, S.W., Ding, Q.H., 2003. $^{40}Ar–^{39}Ar$ and K–Ar dating of the Yixian Formation volcanic rocks, western Liaoning province, China. Geochimica 32, 427–435 (in Chinese with English abstract).

Renne, P.R., Swisher, C.C., Deino, A.L., Karner, D.B., Owens, T.L., DePaolo, D.J., 1998. Intercalibration of standards, absolute ages and uncertainties in $^{40}Ar/^{39}Ar$ dating. Chem. Geol. 145, 117–152.

Robinson, P.T., Zhou, M.F., Hu, X.F., Reynolds, P., Bai, W.J., 1999. Geochemical constraints on the petrogenesis and tectonic setting of the Hegenshan ophiolite, Northern China. J. Asian Earth Sci. 17, 423–442.

Sagong, H., Kwon, S.T., 2005. Mesozoic episodic magmatism in South Korea and its tectonic implication. Tectonics 24. doi:10.1029/2004TC001720.

Sengör, A.M.C., Natal'in, B.A., 1996. Paleotectonics of Asia: fragments of a synthesis. In: Yin, A., Harrison, M. (Eds.), The Tectonic Evolution of Asia. Cambridge University Press, Cambridge, pp. 486–640.

Sengör, A.M.C., Natal'in, B.A., Burtman, V.S., 1993. Evolution of the Altaid tectonic collage and Paleozoic crustal growth in Eurasia. Nature 364, 299–307.

Shao, J.A., Zhang, L.Q., 2002. Mesozoic dyke swarms in the north of Northern China. Acta Petrol. Sin. 18, 312–318 (in Chinese with English abstract).

Shao, J.A., Zang, S.X., Mou, B.L., 1994. Extensional tectonics and asthenospheric upwelling in the orogenic belt: a case study from Hinggan–Mongolia Orogenic belt. Chin. Sci. Bull. 39, 533–537.

Shao, J.A., Zhang, L.Q., Mou, B.L., 1998. Thermo-tectonic evolution in middle and south part of Dahinggan. Sci. China (D) 28, 194–200 (in Chinese).

Shao, J.A., Li, X.H., Zhang, L.Q., Mu, B.L., Liu, Y.L., 2001a. Geochemical conditions for genetic mechanism of the Mesozoic bimodal dyke swarms in Nankou–Guyaju. Geochemica 30, 517–524 (in Chinese with English Abstract).

Shao, J.A., Liu, F.T., Chen, H., Han, Q.J., 2001b. Relationship between Mesozoic magmatism and subduction in Da Hinggan-Yanshan area. Acta Geol. Sin. 75, 56–63.

Shi, G.H., Miao, L.C., Zhang, F.Q., Jian, P., Fan, W.M., Liu, D.Y., 2004. Emplacement age and tectonic implications of Xilinhot A-type granite in Inner Mongolia, China. Chin. Sci. Bull. 49, 723–729.

Smith, P.E., Evensen, N.M., York, D., Chang, M.M., Jian, F., Li, J.L., Cumbaa, S., Russell, D., 1995. Dates and rates in ancient lakes: $^{40}Ar/^{39}Ar$ evidence for an Early Cretaceous age for the Jehol Group, northeastern China. Can. J. Earth Sci. 32, 1426–1431.

Spell, T.S., McDougall, I., 2003. Characterization and calibration of $^{40}Ar/^{39}Ar$ dating standards. Chem. Geol. 198, 189–211.

Sun, D.Y., Wu, F.Y., Li, H.M., Lin, Q., 2001. Emplacement age of the postorogenic A-type granites in Northwestern Lesser Xing'an Ranges, and its relationship to the eastward extension of Suolunshan–Hegenshan–Zhalaite collisional suture zone. Chin. Sci. Bull. 46, 427–432.

Swisher III, C.C., Wang, Y.Q., Wang, X.L., Xu, X., Wang, Y., 1999. Cretaceous age for the feathered dinosaurs of Liaoning, China. Nature 400, 58–61.

Swisher III, C.C., Wang, X.L., Zhou, Z.H., Wang, Y.Q., Jin, F., Zhang, J.Y., Xu, X., Zhang, F.C., Wang, Y., 2002. Further support for a Cretaceous age for the feathered-dinosaur beds of Liaoning, China: new $^{40}Ar/^{39}Ar$ dating of the Yixian and Tuchengzi formations. Chin. Sci. Bull. 47, 135–138.

Tang, K.D., 1990. Tectonic development of Paleozoic fold belts at the north margin of the Sino-Korean craton. Tectonics 9, 249–260.

Tomurtogoo, O., Windley, B.F., Kroner, A., Badarch, G., Liu, D.Y., 2005. Zircon age and occurrence of the Adaatsag ophiolite and Muron shear zone, central Mongolia: constraints on the evolution

of the Mongol–Okhotsk ocean, suture and orogen. J. Geol. Soc. London 162, 125–134.
Uyeda, S., Miyashiro, A., 1974. Plate tectonics and the Japanese islands: A synthesis. Geo. Soc. Am. Bull. 85, 1159–1170.
Van der Voo, R., Spakman, W., Bijwaard, H., 1999. Mesozoic subducted slabs under Siberia. Nature 397, 246–249.
Wang, Y.X., Zhao, Z.H., 1997. Geochemistry and origin of the Baerzhe REE–Nb–Be–Zr super-large deposit. Geochimica 26, 24–35 (in Chinese with English abstract).
Wang, Y.Q., Su, Y.Z., Liu, E.Y., 1997. Regional Strata of Northeast China. China University of Geosciences Publishing House, Wuhan, pp. 1–175 (in Chinese).
Wang, S.S., Hu, H.G., Li, P.X., Wang, Y.Q., 2001a. Further discussion on the geologic age of Sihetun vertebrate assemblage in western Liaoning, China: evidence from Ar–Ar dating. Acta Petrol. Sin. 17, 663–668 (in Chinese with English abstract).
Wang, S.S., Wang, Y.Q., Hu, H.G., Li, H.M., 2001b. The existing time of Sihetun vertebrate in western Liaoning, China: evidence from U–Pb age of zircon. Chin. Sci. Bull. 46, 779–782.
Wang, P.J., Liu, Z.J., Wang, S.X., Song, W.H., 2002. $^{40}Ar/^{39}Ar$ and K/Ar dating of the volcanic rocks in the Songliao basin, NE China: constraints on stratigraphy and basin dynamics. Int. J. Earth. Sci. 91, 331–340.
Wang, F., He, H.Y., Zhu, R.X., Sang, H.Q., Wang, Y.L., Yang, L.K., 2005. Intercalibration of international and domestic $^{40}Ar/^{39}Ar$ dating standards. Sci. China (series D) 49, 461–470.
Wang, F., Zhou, X.H., Zhang, L.C., Ying, J.F., Zhang, Y.T., Wu, F.Y., Zhu, R.X., 2006. Late Mesozoic volcanism in the Great Xing'an Range (NE China): timing and implications for the dynamic setting of NE Asia. Earth Planet. Sci. Lett. 251, 179–198.
Wu, F.Y., Sun, D.Y., 1999. The Mesozoic magmatism and lithospheric thinning in Eastern China. J. Changchun Uni. Sci. Tech. 29, 313–318 (in Chinese with English abstract).
Wu, F.Y., Sun, D.Y., Zhang, G.L., Ren, X.W., 2000a. Deep Geodynamics of Yanshan Movement. Geol. J. China Uni. 6, 379–388 (in Chinese with English abstract).
Wu, F.Y., Jahn, B.M., Wilde, S., Sun, D.Y., 2000b. Phanerozoic crustal growth: U–Pb and Sr–Nd isotopic evidence from the granites in northeastern China. Tectonophysics 328, 89–113.
Wu, F.Y., Sun, D.Y., Li, H.M., Wang, X.L., 2001. The nature of basement beneath the Songliao Basin in NE China: geochemical and isotopic constraints. Phys. Chem. Earth (part A), 26, 793–803.
Wu, F.Y., Sun, D.Y., Li, H.M., Jahn, B.M., Wilde, S., 2002. A-type granites in northeastern China: age and geochemical constraints on their petrogenesis. Chem. Geol. 187, 143–173.
Wu, F.Y., Ge, W.C., Sun, D.Y., Guo, C.L., 2003a. Discussions on the lithospheric thinning in Eastern China. Earth Sci. Front. 10, 51–59 (in Chinese with English abstract).
Wu, F.Y., Walker, R.J., Ren, X.W., Sun, D.Y., Zhou, X.H., 2003b. Osmium isotope constraints on the age of lithospheric mantle beneath the northeast China. Geol. 197, 107–129.
Wu, F.Y., Lin, J.Q., Wilde, S.A., Zhang, X.O., Yang, J.H., 2005a. Nature and significance of the Early Cretaceous giant igneous event in eastern China. Earth Planet. Sci. Lett. 233, 103–119.
Wu, F.Y., Yang, J.H., Wilde, S.A., Zhang, X.O., 2005b. Geochronology, petrogenesis and tectonic implications of the Jurassic granites in the Liaodong Peninsula, NE China. Chem. Geol. 221, 127–156.
Wu, G., Sun, F.Y., Zhao, C.S., Li, Z.T., Zhao, A.L., Pang, Q.B., Li, G.Y., 2005c. Discovery of the Early Paleozoic post orogenic granite in northern margin of the Erguna massif and its significance. Chin. Sci. Bull. 50, 2733–2743.
Wu, G., Zhu, Q., Li, Z.D., Wang, X.J., Wang, H.B., Li, G.Y., Pang, Q.B., 2005d. Geochemical feature and $^{40}Ar/^{39}Ar$ dating of the Mesozoic volcanic rocks in the northern Great Xing'an Range. Abstract of 2005 national meeting of the petrology and geodynamics in China, pp. 127–130 (in Chinese).
Wu, F.Y., Walker, R.J., Yang, Y.H., Yuan, H.L., Yang, J.H., 2006. The chemical-temporal evolution of lithospheric mantle underlying the North China Craton. Geochim. Cosmochim. Acta 70, 5013–5034.
Wu, F.Y., Yang, J.H., Lo, C.H., Wilde, S.A., Sun, D.Y., Jahn, B.M., 2007a. The Heilongjiang Group: a Jurassic accretionary complex in the Jiamusi Massif at the western Pacific margin of northeastern China. Island Arc 16, 156–172.
Wu, F.Y., Han, R.H., Yang, J.H., Wilde, S.A., Zhai, M.G., Park, S.C., 2007b. Initial constraints on the timing of granitic magmatism in North Korea using U–Pb zircon geochronology. Chem. Geol. 238, 232–248.
Xu, Y.G., 2001. Thermal-tectonic destruction of the Archean lithospheric keel beneath the Sino-Korean craton in China: evidence, timing and mechanism. Phys. Chem. Earth 26, 747–757.
Yan, J.Y., Tang, K.D., Bai, J.W., Mo, Y.C., 1989. High pressure metamorphic rocks and their tectonic environment in northeastern China. J. SE Asian Earth Sci. 3, 303–313.
Yang, Z.Z., Meng, Q.C., Gang, J., Han, X.P., 1996. Liaonan Metamorphic core complex. Liaoning Geol. 4, 241–250 (in Chinese with English abstract).
Ye, H.W., Zhang, X.Z., Zhou, Y.W., 1994. The texture and evolution of Manzhouli-Suifenhe lithosphere-study based on features of blues-chist and ophiolites. In: M-SGT geological project group (Ed.), Geological study on the texture and evolution of the Manzhouli-Suifenhe geological section in China. Seismic Publishing House, 73-83.
Yuan, H.L., Gao, S., Liu, X.M., Li, H.M., Gunther, D., Wu, F.Y., 2004. Accurate U–Pb age and trace element determinations of zircon by laser ablation-inductively coupled plasma mass spectrometry. Geostand. Newslett. 28, 353–370.
Zhang, H.F., 2005. Transformation of lithospheric mantle through peridotite-melt reaction: A case of Sino-Korean craton. Earth Planet. Sci. Lett. 237, 768–780.
Zhang, J.H., 2006. Geochronological framework of the Mesozoic volcanic rocks in the Great Xing'an Range, NE China. Master Dissertation, Jilin University, 1−94.
Zhang, Y.P., Tang, K.D., 1989. Pre-Jurassic tectonic evolution of intercontinental region and the suture zone between the North China and Siberian platforms. J. SE Asian Earth Sci. 3, 47–55.
Zhang, L.Q., Shao, J.A., Zheng, G.R., 1998. Metamorphic core complex in Ganzhuermiao, Inner Mongolia. Sci. Geol. Sin. 33, 140–146 (in Chinese with English abstract).
Zhang, X.D., Yu, Q., Chen, F.J., Wang, X.W., 2000. Structural characteristics, origin and evolution of metamorphic core complex in central basement uplift and Xujiaweizi faulted depression in Songliao Basin, northeastern China. Earth Sci. Front. 7, 411–419 (in Chinese with English abstract).
Zhang, J.H., Ge, W.C., Wu, F.Y., Liu, X.M., 2006. Mesozoic bimodal volcanic suite in Zhalantun of the Da Hinggan Range and its geological significance: zircon U–Pb age and Hf isotopic constraints. Acta Geol. Sin. 80, 801–812.
Zhao, G.L., Yang, G.L., Fu, J.Y., Wang, Z., Fu, J.Y., Yang, Y.Z., 1989. Mesozoic volcanic rocks in central and southern Da Hinggan Ling Range, vol. 1. Beijing Science and Technology Publishing House, Beijing, pp. 1–260 (in Chinese with English abstract).
Zheng, J.P., Griffin, W.L., O'Reilly, S.Y., Yang, J.S., Li, T.F., Zhang, M., Zhang, R.Y., Liou, J.G., 2006. Mineral chemistry of peridotites

from Paleozoic, Mesozoic and Cenozoic lithosphere: constraints on mantle evolution beneath Eastern China. J. Petrol. 47, 2233–2256.

Zhou, C.Y., Wu, F.Y., Ge, W.C., Sun, D.Y., Rahman, A.A.A., Zhang, J.H., Cheng, R.Y., 2005. Age, geochemistry and petrogenesis of the cumulate gabbro in Tahe, northern Da Hinggan Mountain. Acta Petrol. Sin. 21, 763–775 (in Chinese with English abstract).

Zhou, M.F., Zhang, H.F., Robinson, P.T., Maipas, J., 2003. Comments on "Petrology of the Hegenshan ophiolite and its implication for the tectonic evolution of northern China" by T. Nozaka and Y. Liu [*Earth Planet. Sci. Lett.* 202 (2002) 89–104]. Earth Planet. Sci. Lett. 217, 207–210.